RNI: DELENG/2005/15153
Publication: 23rd of every month
Posting: 27th/28th of every month at DPSO

No: DL(E)-01/5079/2023-25
Licensed to post without pre-payment U(E) 28/2023-25
Rs.150

www.mycoordinates.org

ISSN 0973-2136

Coordinates

Volume XIX, Issue 2, February 2023

THE MONTHLY MAGAZINE ON POSITIONING, NAVIGATION AND BEYOND

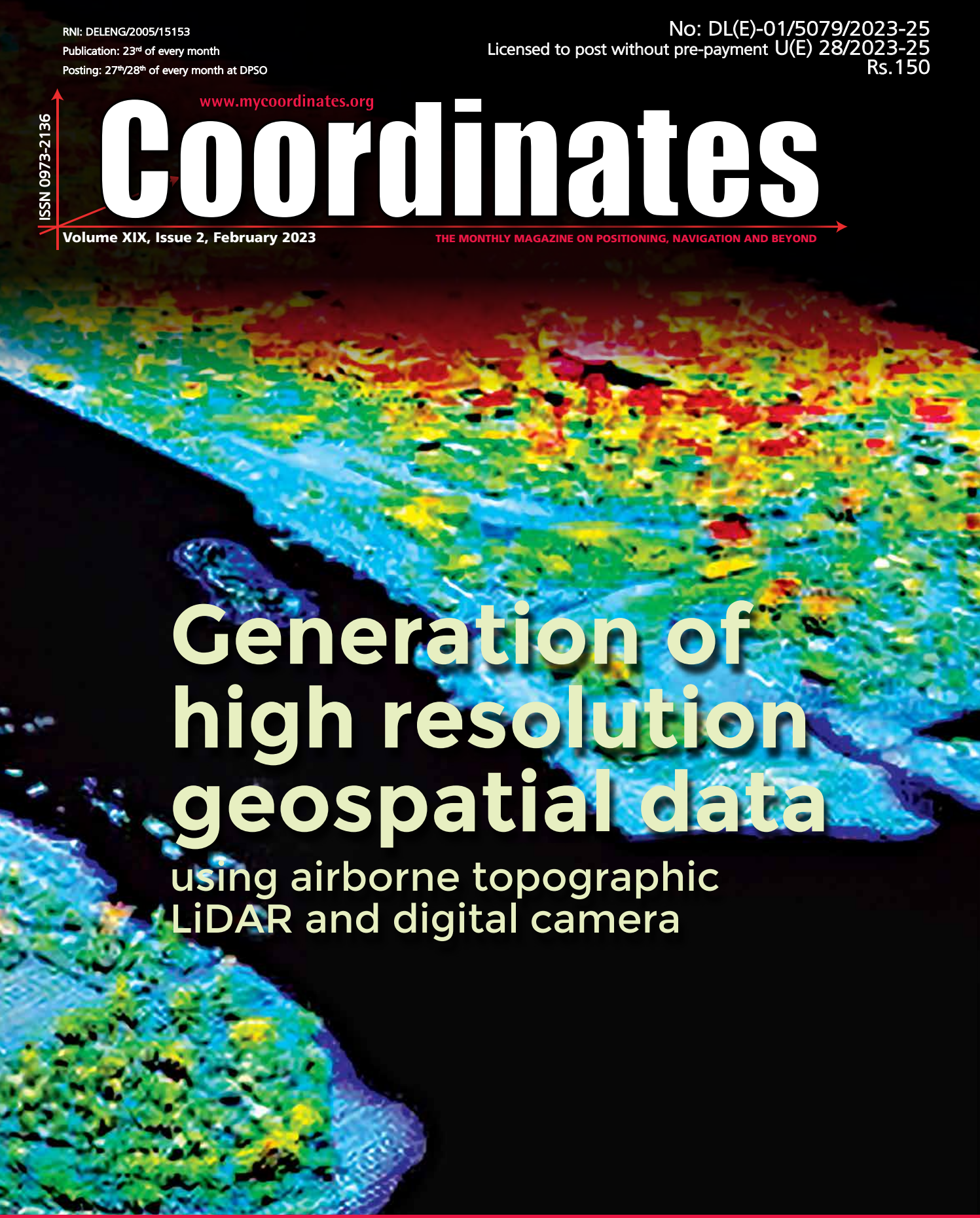

Generation of high resolution geospatial data

using airborne topographic LiDAR and digital camera

Employee location tracking in retail stores

In Coordinates

10 years before...

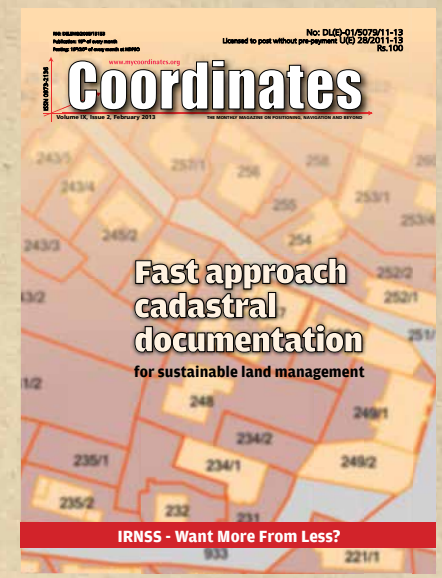

mycoordinates.org/vol-9-issue-2-February-2013

IRNSS – Want More From Less?

Vyasaraj Guru Rao
Accord Software & Systems Pvt Ltd, Bangalore, India

Gerard Lachapelle
Professor of Geomatics Engineering, University of Calgary, Canada

This research performed an analysis with different vectors (locations of satellites), deduced an optimal constellation with slots available to India (ISRO) and yet achieves 60% more coverage (w.r.t availability and thus accuracy) than the existing constellation. From a regional perspective this is a significant improvement where more coverage is achieved with less (without additional) satellites. With this as reference, if additional satellites are added to this constellation in future, availability/ accuracy and in turn robustness (satellite failure) can be addressed.

Fast approach cadastral documentation

Dr Alexander Kohli
Vice-President, Swiss Land Management Foundation, c/o BSB + Partner, Consulting Engineers, Switzerland

The logical consequence of economic development–land consumption–substantiates the need for sustainable land management and cadastre. Successful attempts to direct or manage land consumption or land use can only run on a solid base of a well-maintained digital cadastre which represents the actual situation of property and tenure holdings as well as the Public-Law restrictions (PLR) on land.

Critical developments in land surveying

Brian J Coutts
School of Surveying, University of Otago, Dunedin, New Zealand
Malcolm McCoy
Former President, Institution of Surveyors Australia (ISA) Vekta Pty Ltd, Australia

It is clear that there will need to be a body of knowledge that a land surveyor is expected to have, and that recognition of that body of knowledge is currently through a university education, followed by a period of "training" that is then tested after a period of practice.

Solutions for open land administration

Neil Pullar, Andrew McDowell, Alexander Solovov, Elton Manoku and Maria Paola Rizzo
NRC Land Tenure Team, Food & Agriculture Organization, Rome

The Solutions for Open Land Administration (SOLA) Open Source Software project is a 3 year trust fund project, funded through the Government of Finland and implemented by a project team within the UN FAO. Its aim is to make computerized cadastre and registration systems based on open source software more affordable and more sustainable in developing countries.

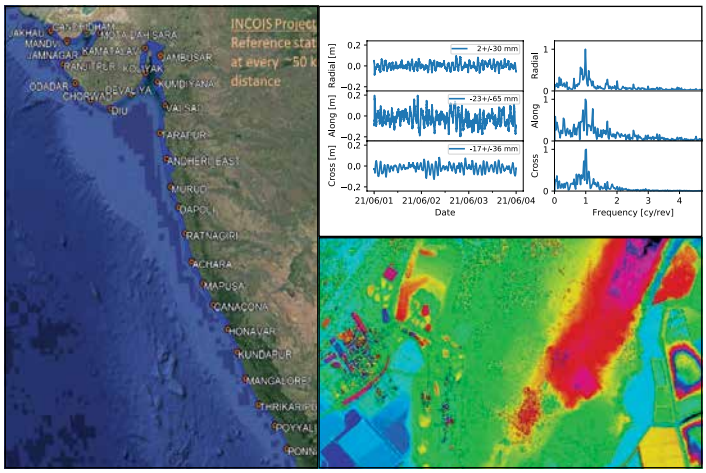

In this issue

Coordinates Volume 19, Issue 2, February 2023

Articles

Generation of high resolution geospatial data using airborne topographic LiDAR and digital camera data B Sadasiva Rao, G Varaprasad Babu, B Laxman, P Srinivasulu, S Muralikrishnan, R S Mahendra, P C Mohanty, Ch Patanjali Kumar and T Srinivasa Kumar **Employee location tracking in retail stores** Caner Guney, Emre Tuncel and Hakan Ulagan 13

Performance assessment of GNSS-based real-time navigation for the Sentinel-6 spacecraft Oliver Montenbruck, Florian Kunzi and André Hauschild 16

Columns

Old Coordinates 2 **My Coordinates** Editorial 4 **News** GIS 26 GNSS 28 Imaging 28 UAV 30 LBS 30 Industry 32

Mark Your Calendar 34

This issue has been made possible by the support and good wishes of the following individuals and companies
André Hauschild, B Laxman, B Sadasiva Rao, Caner Guney, Ch Patanjali Kumar, Emre Tuncel, Florian Kunzi, G Varaprasad Babu, Hakan Ulagan, Oliver Montenbruck, P C Mohanty, P Srinivasulu, R S Mahendra, S Muralikrishnan and T Srinivasa Kumar; SBG System, and many others.

Mailing Address
A 002, Mansara Apartments
C 9, Vasundhara Enclave
Delhi 110 096, India.
Phones +91 11 42153861, 98102 33422, 98107 24567

Email
[information] talktous@mycoordinates.org
[editorial] bal@mycoordinates.org
[advertising] sam@mycoordinates.org
[subscriptions] iwant@mycoordinates.org
Web www.mycoordinates.org

Coordinates is an initiative of CMPL that aims to broaden the scope of positioning, navigation and related technologies. CMPL does not neccesarily subscribe to the views expressed by the authors in this magazine and may not be held liable for any losses caused directly or indirectly due to the information provided herein. © CMPL, 2023. Reprinting with permission is encouraged; contact the editor for details.

Annual subscription (12 issues)
[India] Rs.1,800* [Overseas] US$100*
*Excluding postage and handling charges

Printed and published by Sanjay Malaviya on behalf of Coordinates Media Pvt Ltd
Published at A 002 Mansara Apartments, Vasundhara Enclave, Delhi 110096, India.
Printed at Thomson Press (India) Ltd, Mathura Road, Faridabad, India

Editor Bal Krishna
Owner Coordinates Media Pvt Ltd (CMPL)

This issue of Coordinates is of 36 pages, including cover.

A grim reminder

On February 6th, when the earth trembled for a few seconds,

Cities collapsed in southern Turkey and northern Syria,

Thousands perished.

It happened not for the first time and nor will be the last,

But stories unfold in the similar manner in most of the cases.

A repeated reminder to all of us sitting on seismic zones,

That we may be the next.

God forbid.

Bal Krishna, Editor
bal@mycoordinates.org

ADVISORS Naser El-Sheimy PEng, CRC Professor, Department of Geomatics Engineering, The University of Calgary Canada, George Cho Professor in GIS and the Law, University of Canberra, Australia, Professor Abbas Rajabifard Director, Centre for SDI and Land Administration, University of Melbourne, Australia, Luiz Paulo Souto Fortes PhD Associate Professor, University of State of Rio Janeiro (UERJ), Brazil, John Hannah Professor, School of Surveying, University of Otago, New Zealand

Generation of high resolution geospatial data using airborne topographic LiDAR and digital camera data

Data has been utilised in generation of tsunami models at local scale for different magnitudes of earthquakes, preparation of multi hazard vulnerability maps for oceanogenic disasters, to assess disasters at micro-level and planning the mitigation

B Sadasiva Rao
National Remote Sensing Centre (NRSC), Hyderabad, India

R S Mahendra
Indian National Centre for Ocean Information Services (INCOIS), Hyderabad, India

G Varaprasad Babu
National Remote Sensing Centre (NRSC), Hyderabad, India

P C Mohanty
Indian National Centre for Ocean Information Services (INCOIS), Hyderabad, India

B Laxman
National Remote Sensing Centre (NRSC), Hyderabad, India

Ch Patanjali Kumar
Indian National Centre for Ocean Information Services (INCOIS), Hyderabad, India

P Srinivasulu
National Remote Sensing Centre (NRSC), Hyderabad, India

T Srinivasa Kumar
Indian National Centre for Ocean Information Services (INCOIS), Hyderabad, India

S Muralikrishnan
National Remote Sensing Centre (NRSC), Hyderabad, India

Introduction

Airborne topographic LiDAR scanner (ALS) integrated with medium format single CCD digital camera (MFDC) is utilised off late very extensively in large scale geospatial database generation projects to produce precise high resolution (HR) DTMs. LiDAR has capability of delivering 3D point clouds of terrain and object surfaces (DSM &DTM) height information in short duration of time with high spatial density to an accuracy of decimeter. MFDC data is used to generate large scale (LS) planimetric maps from orthoimages (Gopala Krishna et al. 2013). National Remote Sensing Centre (NRSC), ISRO has delivered the HR DTMs, LS Topo maps, and 2.5D building database, which were produced using data acquired by ALS LiDAR sensor and Medium format digital camera along the Indian mainland coastline covering ~5000 km with an extent of area ~24000 sq. km (fig:1) having inland coverage of 2km from the coast including major estuary, creeks for INCOIS organisation (Indian national centre for ocean information services), GOI under Ministry of Earth sciences located at Hyderabad, India. This data is utilised at the Tsunami warning centre as one of the inputs in building Tsunami inundation models for different earthquake scenarios possible

on the east coast(Andaman-Sumatra subduction zone, Bay of Bengal sea) and west coast(the Makran subduction zone, Arabian sea (Shailesh Nayak et al. 2008). Also utilised these datasets to prepare and update multi-hazard (Tsunami, Cyclones, floods) vulnerability maps representing vulnerability, risk, and hazard information together.

Tsunamis and cyclonic storms generate massive water wave surges at the sea coast in different amplitudes. These surges cause seawater flooding into the land as much as 1-2 km or even more, resulting in loss of human life and damage to property. INCOIS has developed Tsunami & storm surge models to predict the inundation along the Indian coast using HR DTMs and other inputs (Srinivasa Kumar et al., 2012). These models help in the preparation of geospatial information, which indicates the potential areas which are affected due to tsunami and cyclone inundation at the cadastral level (Mahendra et al. 2011 & 2010, Srinivasa Kumar et al. 2010). These inputs help disaster management teams of central-and state-level departments to utilise in mitigation planning, rescue and evacuation operations.

The accuracy of inundation model prediction is directly related to the quality of the topography data apart from other inputs. To provide the inundation information at cadastral/ parcel level for coastal areas covering a large area with flat lands with fewer undulations and cluttered with small buildings requires high-resolution topographic data sets and large-scale planimetric information. High-resolution data acquired with decimeter accuracy in position and elevation by LiDAR and MFDC sensors were used in delivering large-scale topographic and planimetric data in this project. Seamless Hydro enforced and Hydro conditioned DTMs in MSL datum with elevation accuracy of 0.35m having grid spacing of 5m and contour with 1m intervals were generated to utilise them in inundation modelling for the entire mainland of Indian coast. Produced Large scale planimetric maps in 1:5000 scale (generated from 0.50m GSD orthoimages produced from MFDC digital camera images integrated with LiDAR sensor) having information layers of built-up area, transportation network, communication & power infrastructure, hydrographic features etc., Also generated 2.5D building database, accurate to 1m height which helps in identifying relief shelters, buildings. This building database is also used to simulate inundation by different water levels to plan rescue operations in case of evacuation.

Indian coast is covered with flat to highly undulating terrain with various landforms such as Sand beaches, Mudflats, marshy lands, rocky areas, Mangroves, agricultural farms, aquaculture farms and small villages to urban areas. Acquisition of topographic data optimally with LiDAR, which is operated in the NIR region at 1064nm wavelength where water absorbs the incident energy completely (land covered with waterbodies and wetlands) without sun glint, without dead zones in high urban areas using aircraft in a narrow corridor of 2 km width along the coast throws up various challenges to planning, acquisition, ground teams. This article covers how LiDAR technology and photogrammetry are utilised in the realisation of seamless HR DTM, large-scale 2D geospatial data and 2.5D building database for such complex terrain and land features and its end application for Indian coast.

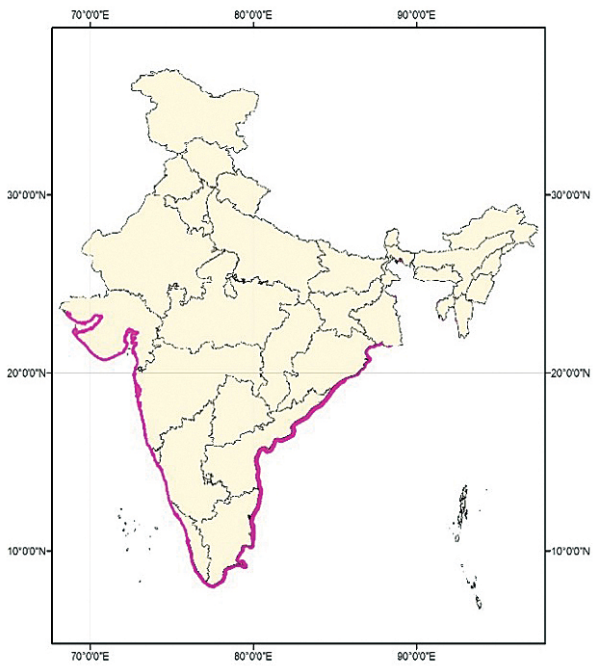

Fig 1 : LiDAR survey area

LiDAR survey planning and acquisition

Flight planning

The total project area to be surveyed is medium in size (~24000 sq. km). Even though the area to be acquired appears to be less in terms of numbers, the area distribution is with a very narrow region of 2kms along the coast, having many bends and discontinuities due to creeks and rivers. To generate seamless LiDAR DTM, a LiDAR survey was planned to cover in several blocks (small areas of near to rectangular polygons) with overlap. Ensured 10% of overlap between block to block during planning. Tie flight lines were also planned to ensure the geometric fidelity of data. Finding the features which are required to tie the blocks is difficult as 40% of the area is covered with sand / beaches and 10% marshy/wetlands. Hence extra area with varied buffer to AOI is taken, so that land features are available to generate tie points/lines (fig:2). To geo-reference the LiDAR data to the decimeter accuracy by using direct geo-referencing (DG) technique, planned boresight calibration flights before commencing the acquisition over calibration sites located at NRSC, Hyderabad along with other system health checks regularly to ensure the overall system performance. Configured the LiDAR sensor and digital camera to acquire both the data simultaneously along with other reference positioning

systems, GPS and IMU. Direct geo-referencing of LiDAR data & camera data is carried out using the EO parameters derived from GPS & IMU integrated positioning data. Orientation of Camera data with EO by DG provides positional accuracy of 2-3 pixels. However, sub-pixel accuracy in position is required to generate seamless orthoimages and to maintain the position of

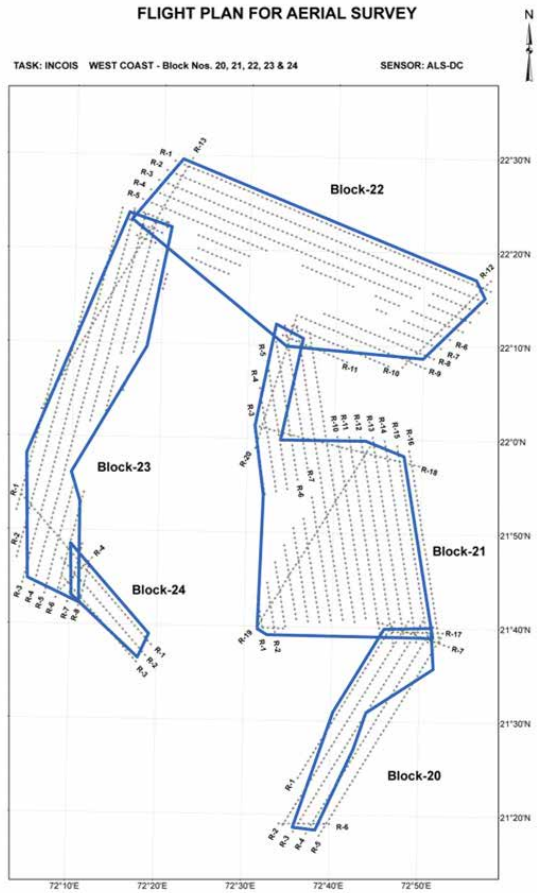

Fig 2 : Flight plan – part of survey area showing flight lines with tie lines

Fig 3 : Geodetic GPS receiver – Base station

planimetric features in the camera with DTM height information. To meet this challenge of geo-referencing of LiDAR point clouds with images precisely, full control points from LiDAR data were planned optimally. Control points collection over small agricultural bunds, edges of painting marks, small bushes in case of remote /vegetative areas etc., from LiDAR data was devised.

Acquisition of data in wide strips reduces the number of flight lines to be acquired and this inturn helps in processing of data with less effort and time. To optimise the flight lines, which are required to cover the entire survey area, including tie lines, a flying height of 3000m was planned to suit the requirement of height accuracy & point spacing with the maximum wide swath possible for each run. Planned 50 deg field of view (FOV) of laser scanner by considering all the requirements said above with 10-15% side lap between flight lines to get optimum flight lines(fig:2).

Ground surveys

Direct geo-reference of both LiDAR & DC image data require exterior orientation parameters and these are derived using post-processed airborne kinetic GPS (KGPS) & IMU data. It is required positional accuracy of 10-15 cm and 0.005deg attitude accuracy to meet the sub-meter location geolocation accuracy of both the data sets, i.e. LiDAR & camera. Kinematic GPS positioning accuracy is poorer due to inherent errors present in data. To remove the errors and improve the accuracy of kinematic GPS data, differential GPS processing is carried out during post-processing by using static GPS data collected on the ground simultaneously during data acquisition. Static GPS data is recorded at 2Hz in the field with close baseline separation. Operated GPS base station during data acquisition optimally along the survey area at 50km spacing as shown in fig: 3 and 4.

Geo-referenced LiDAR data by kinematic GPS data is with respect to the WGS84 ellipsoid coordinate system. To derive the hydrologically corrected DTMs with reference to MSL datum from LiDAR data need precise geoid undulations' N' data which is accurate to 5-10cm. As India does not have geoid undulations to the accuracy of sub decimeter, field methods are employed in this task. In the field, WGS84 height (h) and MSL height (H) is collected at the exact location using geodetic GPS & levelling instrument, respectively, to derive geoid height. The geometric method (N=H-h) is used in the derivation of geoid undulations. In field, the geoid undulations data (h, H) is collected at the regular spacing of about 10km. SOI (Survey of India) established a sparse GT BM network with varying spacing available across India. Those GT BMs were taken as a reference to extend the levelling network by traversing several km (~8000 km) along the coast to collect MSL heights at selected locations. MSL heights are collected on flat surfaces such as platforms, the centre of the road where culverts exist, playgrounds, and open lands. GPS height data collection in the field has been entirely avoided by implementing a novel approach of collecting from LiDAR point's average height at flat

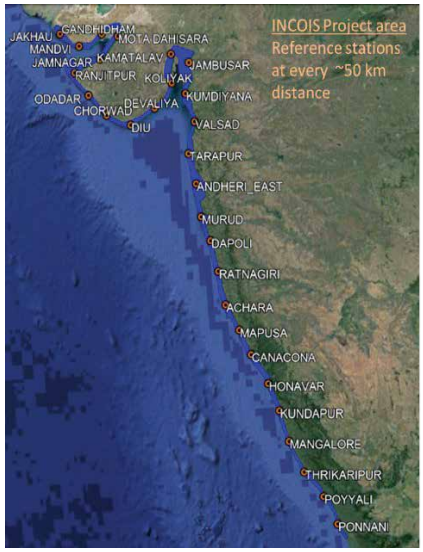

Fig 4: Distribution of GPS ground stations

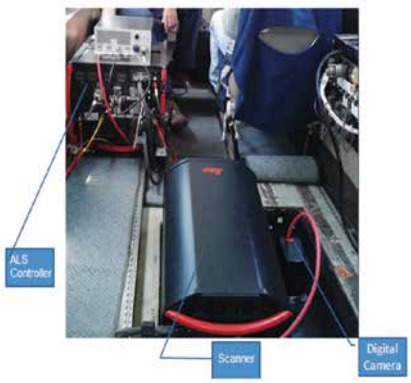

Fig 5: ALS70 & RCD30 Sensors

surface in WGS84 heights instead of using a GPS instrument in field. This methodology has not only reduced the field efforts and contributed in removing the bias errors present in LiDAR data.

Acquisition

Acquired the entire coastal area of ~24000 sq. km in a duration of 10 years. During this period, LiDAR sensors and camera technologies have been changed in terms of accuracy, point spacing, positioning systems, camera total number of pixels, GSD etc. During the span of the entire data acquisition period, three models of LiDAR sensors & cameras were inducted. LiDAR sensor ALS50, ASL50-II, ALS70 and cameras spectrum, rcd105, and rcd30 were used during acquisition.

Technologies have been improved from ALS50 to ALS70 fig (5) in terms of pulse repetition frequency of 50 kHz to 500 kHz, i.e. ten times. Mission planning and sensor controlling, pre-processing software have also been improved. These technological transformations in sensors performance in terms of PRF, mirror scan rate, and range accuracies have helped in acquiring the data optimally. Adoption of tightly coupled systems in place of loosely coupled systems enabled to reduce the turn time in flights. Improvements in high PRF enabled acquisition data at higher point density from the same altitude.

Performance checks and boresight calibration is required to be carried out for each installation of LiDAR and camera prior to the acquisition of data to ensure quality data. LiDAR and camera sensor's critical parameters and their performance were evaluated by conducting flights over calibration sites in and around Hyderabad city. Test flights were conducted at project flying height over calibration site to check the positional accuracies are meeting the planned requirements. Flying over project site was carried out mostly after the post-monsoon season to acquire the cloud-free images and LiDAR data with minimal flying efforts.

Data processing

To generate a seamless dataset for the survey area, which is spread across several longitudes from 68° to 88° and falls in UTM zones of 42 to 44, requires initial planning to avoid edge matching errors during data pre-processing, datum conversions and features extraction. Processing of LiDAR and camera data which are in sensor coordinates to map coordinates and conversion of ellipsoid heights to MSL heights, requires several transformations. The following steps were followed in the processing of LiDAR and digital camera data sets to generate HR DTMs in MSL datum with 35cm accuracy, 2D planimetric geospatial data in 1:5000 scale with an accuracy of 0.25mm of map scale and contours of

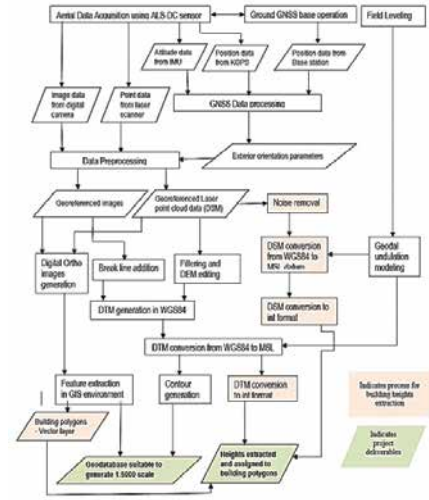

Fig 6: Process flow of LiDAR project

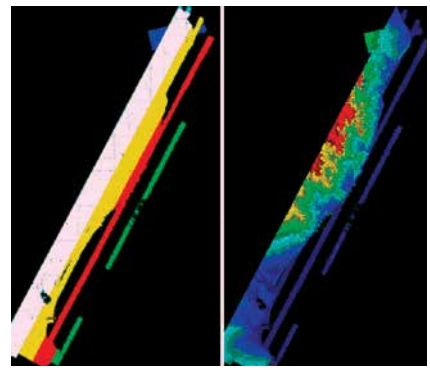

Fig 7 : individual flight lines of LiDAR data

1m with 1/3rd accuracy as per ASPRS standards and extraction of building roof heights with 1m accuracy above ground. The flowchart (fig:6) shows the interaction between different processes during the LiDAR project life cycle.

LiDAR data processing steps

- *Calibration of boresight angles*
- *Lever arm measurements*
- *Geo-referencing*
- *Strip adjustment*
- *Ground classification*
- *Incorporation of 3D brake lines*
- *Geoid undulations modelling*
- *MSL data conversion*

Camera data processing steps

- *Raw to image data with Radiometric corrections*
- *EO parameters generation*
- *Boresight angles calibration*
- *Orthoimages generation*
- *2D Geodatabase generation.*

Boresight-Calibration: Misalignment angles (Δroll, Δpitch, Δkappa) between laser scanner and IMU governs the final accuracy significantly. Not accounting for these angles may induce significant positional errors in meters in some cases (JagannadhaRao et al., 2013). Hence misalignment angles are to be determined very accurately. In the determination of these values, the field boresight calibration method is carried out using the data collected over the flat and slopped surface area in a particular pattern depending on the type of error to be computed. Flight lines over flat surfaces flown in opposite are used to determine roll error, flight lines acquired in opposite directions across over sloped surfaces are used to determine pitch error and to obtain heading error; parallel flight lines are used. These values are to be determined with accuracy better than 0.001 radians. Inclusion of spatial separation (lever arms) distance between different sensors, i.e. IMU and laser scanner and IMU and GPS, is also required during the computation of position accurately. These values (ΔX, ΔY, ΔZ) are determined in the field very precisely using ground instruments such as total station in less than 1cm error.

These calibration flights are carried out for each installation to determine misalignment values apart from verification of other system parameters, viz. encoder latency, torsion angle of scanner shaft, laser range error bias due to electronics delay. LiDAR data which is corrected for all the above systematic errors, are verified against ground control points which are collected over a flat surface (airport runway) to determine absolute accuracy. Seventy control points spread across uniformly on an airport runway of a 2km stretch located at Hyderabad are used to verify absolute accuracy (fig:8).

Camera data pre-processing: Similarly, the camera is also to be calibrated for boresight angles and lever arms. During pre-processing stage i.e conversion of raw camera data to the image, radiometric calibration coefficients are applied to remove the CCD non-uniformity and camera lens distortions coefficients and principal point offset are applied to remove correcting geometric distortions. Subsequently, exterior orientation parameters which are required for orientation and geo-referencing of camera data are deduced using kGPS and IMU combined positional data.

LiDAR data pre-processing: Calibration values determined, i.e. misalignment angles and lever arms, range errors from test flights are applied on data acquired over surveyed data during geo-referencing of laser data. The ultimate objective of LiDAR data processing is the generation of seamless data sets (fig: 7&9). LiDAR data which is acquired in multiple days, have positional errors at side overlap regions due to geo referencing errors induced by varying kGPS positional accuracy. The quantum of positional error depends on the geometry of satellites which varies from time to time with respect to location. The planimetric and height accuracy of LiDAR points differs from sortie/flight to flight due to these GPS errors. Hence there are position errors exist between each flight line overlap in the order of decimeter (positional variation can be observed at the overlapping region of flight lines). To determine these variations between flight lines and minimise the errors, tie flight lines are also acquired. These tie lines connect all the regular flight lines flown together parallel to each other. Critical planning is required to connect regular lines optimally during flight planning. These tie flight lines help in strip adjustment process to determine positional, angular and scale errors present in data for each flight line. To compute the positional errors, Tie lines/tie patches are generated using the least squares fitting method at the common features present in overlap regions and side laps. Using the tie lines identified for different features, differences in positions, rotations and scale are computed. The computed values are used to adjust the LiDAR flight lines together to generate seamless data with 1 to 2 cm.

Average dz	-0.012
Minimum dz	-0.158
Maximum dz	+0.093
Average magnitude	0.050
Root mean square	0.061
Std deviation	0.061

Fig 8 : LiDAR data accuracy (m)

DTM generation: To generate DTM from LiDAR point cloud, bare earth points pertaining to terrain have to be separated out (fig: 10). Also, ground points are to be added where ever points are missing along the edges of features such as stream centerlines, canal edges and also points are to be removed where

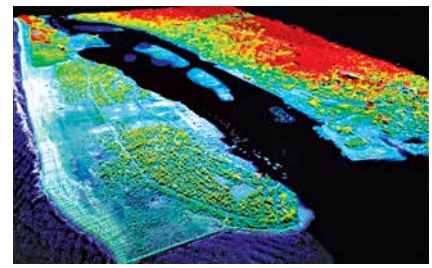

Fig 9: LiDAR point cloud

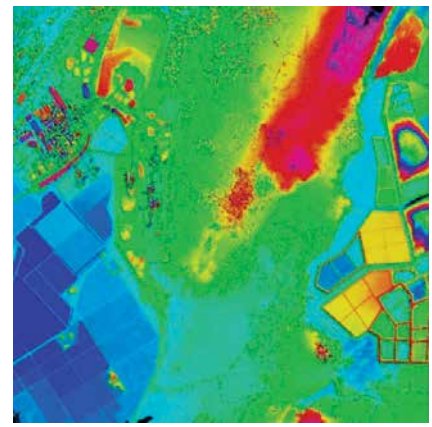

Fig 10: DTM

Fig 11: Location of MSL height

hydrographic features are passing below the cultural features such as roads, rail, and culverts. To obtain terrain points from the point cloud, a progressive densification classification algorithm is used. This algorithm works with 75% to 85% accuracy in flood plain flood-prone areas where most of the lands are flat to moderate and have agricultural crops and short vegetation such as scrubs. The reaming points are either unclassified or misclassified. Usually, classifying the unclassified points, misclassified points, and the addition of extra points in the form of break lines are done manually. This process consumes a lot of processing time and it is a bottleneck in the generation of the DTMs in quick time.

DTMs generated by the above process are in the WGS84 datum, and transformation to the MSL datum is required to make them hydrologically enforced and conditioned. To convert LiDAR DTMs which are in WGS84, to MSL datum, geoid undulations data which is better than decimeter, is required. India does not have such precise geoid information for the

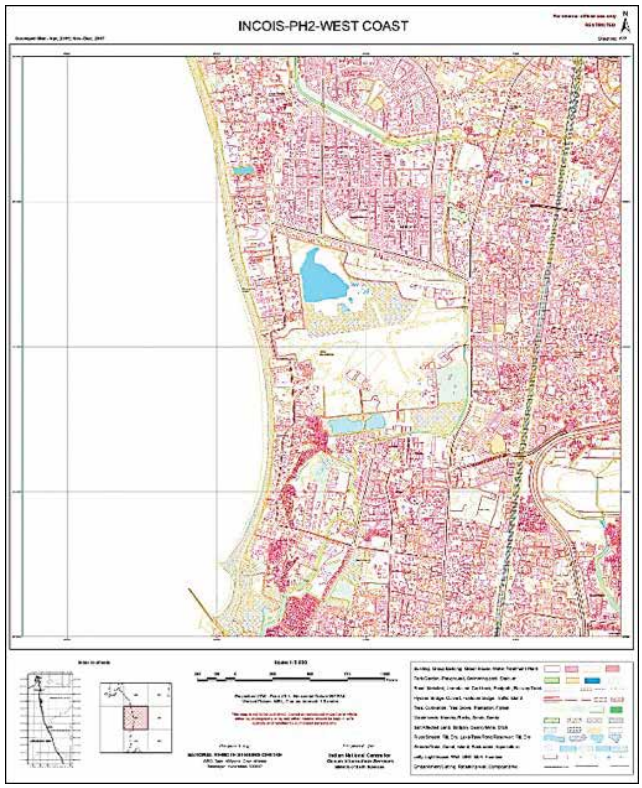

Fig 12: Basemap with contours

Fig 13 : 2.5D buildings – Mangalore city

The products generated from ALS & MFDC data sets i.e DTM, orthoimages, 2.5D buildings were used in various applications by INCIOS along with other ancillary data sets

project survey area (along the coast). Hence data collected using the ground method was employed. Geoid undulation is derived by subtracting the terrain height collected at the exact location in WGS84 datum and MSL datum. The field method involves enormous effort and costs to obtain levelling and GPS data. In this project, MSL heights were collected using levelling instrument, and WGS84 heights were collected in the lab from LiDAR data. Optimised the collection of WGS84 heights with GPS by establishing a new approach in which WGS84 Heights are collected from LiDAR data itself, where flat land is present. As identification and collecting WGS84 height at a particular LiDAR footprint location and collecting MSL height exactly over the LiDAR point is difficult, flat ground patches available in the field are used for MSL height. Flat patches such as platforms, playgrounds, flat Road centers, open Grounds etc., are opted for during data collection (fig:11). This approach has reduced the field component effort and enabled the reducing project timelines. DTMs which are corrected in all aspects are stored in Geotiff format with coordinate system of UTM to use in final hydro modelling, as well as generated orthoimages from digital camera data which is oriented very precisely to one-third of pixel by using photogrammetric block adjustment methods at 50 cm resolution. Orthoimages which are corrected for terrain relief were used further to capture 2D planimetric information of cultural, natural features position, boundaries at 1 in 5000 scale by visual interpretation methods digitally in GIS environment as it requires cartographic quality and positional accuracy of 0.25mm of map scale(fig:12).

To extract rooftop heights of 2.5D buildings (fig:13) with respect to MSL and AGL(above ground level), building vector layer captured from MFDC orthoimage, LiDAR DSM and DTM are used as input(Sadasiva Rao et al., 2013). A tool was developed in-house to automatically extract the MSL height and AGL height of the building using the raster DSM and DTM. For each 2D building boundary, a height value is assigned based on the metrics (Majority and Median) computed using DTM and DSM pixels within the footprint. To deduce rooftop heights with respect to MSL datum, the majority of the DSM pixels height is assigned as it takes care of roof height errors induced due to the presence of adjacent overlapping vegetation, parapet walls, lift rooms and water tanks etc. The median of the pixels height of DTM is used to compute the terrain heights within the footprint as it

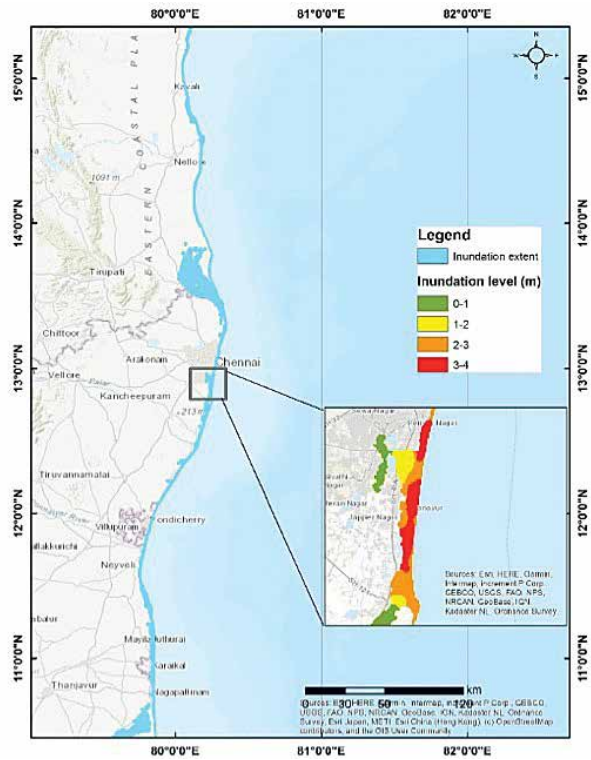

Fig 14 : Tsunami Inundation Map east coast, parts of the southern Chennai coast are shown in inset zoomed map

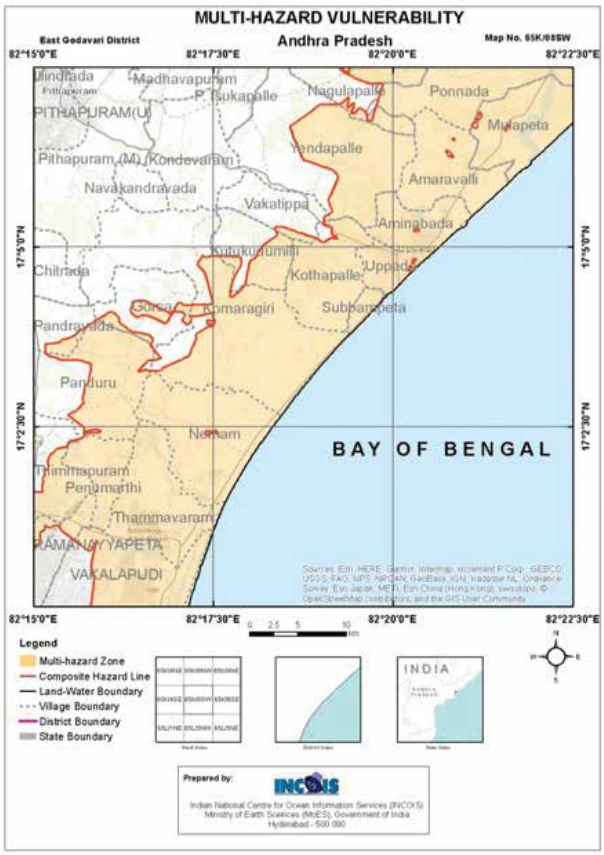

Fig 15 : Sample MHVM map on 1:25000 scale showing the parts of Andhra Pradesh coast

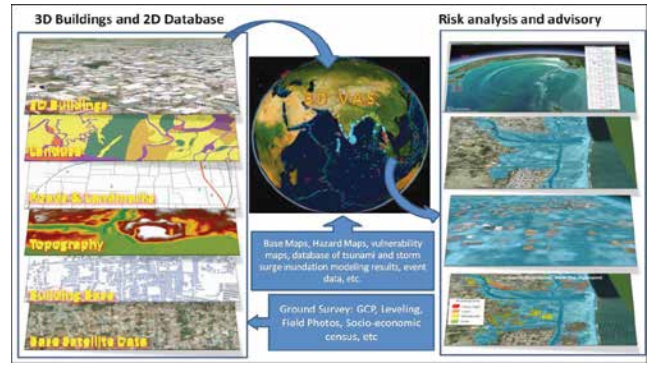

Fig 16 : 3D VAS integrated with 3D/3D geospatial data and tsunami risk assessment

takes care of the slope of the terrain. AGL height is derived by subtracting DTM median heights from DSM majority heights.

Data utilisation

The products generated from ALS & MFDC data sets i.e DTM, orthoimages, 2.5D buildings were used in the following applications by INCIOS along with other ancillary data sets.

Tsunami Inundation modelling : The high-resolution topographic data from Airborne LiDAR and Cartosat-1 satellite DEM were merged with the available coastal bathymetry as an input for the coastal inundation modelling. The 26 December 2004 Indian ocean tsunami generated due to Mw 9.3 magnitude earthquake scenario was simulated on these data using the seismic parameters (Usha et al 2012; Iyyappan et al., 2018). The simulation was carried out in the ADCIRC model by providing the initial condition (water displacement) estimated as per Legg et al. (2004). The results of the Tsunami inundation of the east coast of India are provided in Fig14. The different run-up heights on the coast were recorded depicting the risk of tsunami exposure in the coastal zones. These maps help in the planning of tsunami disaster.

Multi-hazard Vulnerability Mapping (MHVM): The purpose of multi-hazard vulnerability mapping (MHVM) is to identify the most vulnerable and high-risk areas due to oceanogenic disasters. The multi-hazard mapping was carried out using the parameters of sea level change, shoreline change rate, elevation contours derived from ALS and Carto-DTM, extreme water level from tide gauges and the return periods (Mahendra et al., 2010, 2011 & 2021). These parameters were synthesized to derive the composite hazard line. These maps represent the coastal inundation caused due to Tsunami, cyclone, flood. The hazard and vulnerability maps are highly useful in coastal zone planning in order to prepare for disaster events and manage the situation during the disaster. These maps are also useful for future developments activates as well. This MHVM mapping was carried out for the entire mainland of India on 1:25000 scale. An atlas comprising 929 maps was prepared. A sample map of the atlas was given in Fig15.

3D GIS Mapping: The geo spatial database generated using the ALS and digital camera images data were integrated into the 3D/2D data visualization and analysis system (3DVAS) desktop application. This 3DVAS application is integrated with the terrain database generated using DTM draped with aerial images. Further, building bases provided with the building height were used to visualize in the 3D GIS environment based on their respective heights. This provides a virtual 3D view of the entire Indian mainland coast. The major purposes of 3D GIS are to visualize and effectively communicate the inundation threat at the street level and to plan evacuation routes. 3DVAS can also simulate tsunami inundation and on-the-fly generate the building level risk maps. Example images of 3DVAS integrated with 3D GIS data and inundation modelling capability are provided in Fig16 .The datasets generated using the ALS topography and orthoimageries are proved to be highly useful for the micro-level disaster assessment and planning.

Conclusions

Datasets acquired from Airborne lidar and digital camera enabled to generate high resolution digital terrain models with an accuracy of 35cm, large scale maps in 1:5000 scale and 2.5D building database for narrow corridor of 2km along the entire Indian main land coast of ~5000 km for an extent of ~24000 sq.km covered with complex features and terrain.

Data has been utilised in generation of tsunami models at local scale for different magnitudes of earthquakes, preparation of multi hazard vulnerability maps for oceanogenic disasters, to assess disasters at micro-level and planning the mitigation.

References

Gopala Krishna PVSSN et al. 2013. Generation of high resolution dem for inundation studies using airborne lidar, ISPRS workshop, WG VIII/1, WG IV/4.

Iyyappan M, Usha T, Ramakrishnan SS, Srinivasa Raju K, Gopinath G, Chenthamil Selvan S, Dash SK and Mishra P. (2018) Evaluation of tsunami inundation using synthetic aperture radar (SAR) data and numerical modeling. *Nat Hazards* 92, 1419–1432. https://doi.org/10.1007/s11069-018-3257-4.

Jagannadha Rao CVKVP, et.al 2013. Airborne lidar data characteristics - issues and solutions, ISPRS workshop, ISPRS WG VIII/1, WG IV/4

Kulp, S.A., Strauss, B.H. 2019. New elevation data triple estimates of global vulnerability to sea-level rise and coastal flooding. Nat Commun 10, 4844

Legg MR, Borrero JC, and Synolakis CE (2004) Tsunami hazards associated with the Catalina Fault in southern California. Earthq Spectra 20(3):917–950. https://doi.org/10.1193/1.1773592

Mahendra RS et al. 2010. Coastal Multi-Hazard Vulnerability Mapping: A Case Study Along The Coast of Nellore District, East Coast of India Italian Journal of Remote Sensing - 2010, 42 (3): 67-76

Mahendra RS, Mohanty PC, Bisoyi H, Srinivasa Kumar T, Nayak S 2011. Assessment and management of coastal multi-hazard vulnerability along the Cuddalore—Villupuram, east coast of India using geospatial techniques. Ocean and Coastal Management 54(4):302–311

Mahendra, R.S., Mohanty, P.C., Francis, P.A., Sudheer Joseph, Balakrishnan Nair T. M. and Srinivasa Kumar T. 2021. Holistic approach to assess the coastal vulnerability to oceanogenic multi-hazards along the coast of Andhra Pradesh, India. *Environ Earth Sci,* 80, 651. https://doi.org/10.1007/s12665-021-09920-z

Mahendra, R.S., Mohanty, P.C., Srinivasa Kumar, T., Shenoi, S. S. C., and Shailesh Nayak. 2010. Coastal Multi-hazard Vulnerability Mapping: A Case Study along the coast of the Nellore District, Andhra Pradesh, East Coast of India. *Italian Journal of Remote Sensing*: Vol. 42, Issue 3, pp. 67-76. https://doi.org/10.5721/ItJRS20104235

RS Mahendra et al. 2011. Assessment and management of coastal multi-hazard vulnerability along the Cuddalore Villupuram, east coast of India using geospatial techniques Ocean & Coastal Management 54 (2011) 302-311

SadasivaRao.B et.al 2013. Generation of 2.5D buildings using airborne lidar and medium format digital camera data for Indian coast, ISPRS workshop, ISPRS WG VIII/1, WG IV/4

Shailesh Nayak et al. 2008. Addressing the Risk of Tsunami in the Indian Ocean, Journal of South Asia Disaster Studies, Vol. 1 No. 1 November (2008) 45-57.

T. Srinivasa Kumar et.al 2010. Coastal Vulnerability Assessment for Orissa State, East Coast of India, Journal of Coastal Research vol.26 no. 3, 523–534.

T. Srinivasa Kumar et.al 2012. Successful monitoring of the 11 April 2012 tsunami off the coast of Sumatra by Indian Tsunami Early Warning Centre, Current Science · October(2012)

Usha T, Ramanamurthy MV, Reddy NT, Mishra P (2012) Tsunami vulnerability assessment in urban areas using numerical model and GIS. Nat Hazards 60:135–147. https://doi.org/10.1007/s11069-011-9957-7

Acknowledgements

The authors would like to acknowledge the support provided in realisation of the project by former Directors of NRSC viz. Shri.Santanu Chowdhury, Dr YVN Krishna Murthy ,Dr V K Dhadwal, Dr V Jayaraman and Dr K Radhakrishnan . Direction and guidance provided by former NRSC Deputy Director, Sri Raghu Venkataraman , ASDM&OA are acknowledged. The Data acquisition, LiDAR Data processing, Ground surveys, Flight planning, Quality Assurance teams and their Heads contributions are duly acknowledged.

Employee location tracking in retail stores

In this study, an innovative hybrid solution is proposed that will bring a different approach to personnel monitoring in a store that will increase productivity in the retail industry

Caner Guney
Istanbul Technical University, Faculty of Civil Engineering, Department of Geomatics Engineering, Istanbul, Turkey

Emre Tuncel
Opthema Teknoloji, Istanbul, Turkey

Hakan Ulagan
Opthema Teknoloji, Istanbul, Turkey

Abstract

Indoor Positioning System generally uses radio signals, visual data or other types of sensor data to determine where assets such as people and objects are located. There are many different indoor solutions and products used in different application areas from smart transportation in smart cities to contact tracking, location-based games to retail. The offered solutions and/or systems by companies for indoor localization, indoor navigation with context-aware provide different accuracy, reliability, installation and maintenance costs according to the techniques and technologies chosen for the purpose. In this study, an innovative hybrid solution is proposed that will bring a different approach to personnel monitoring in a store that will increase productivity in the retail industry. Within the scope of the study, the indoor location determination process will be carried out by using radio frequency and image data together. Map and/or trajectory fusion will be used to integrate different types of results from different sensors. Spatial decision support approach will be used in directing the salesperson to the busy areas in the store.

Introduction

The retail industry pays attention to every detail regarding its customers in order to increase its profitability rates. Many technological approaches are used effectively in the retail marketing, such as store cards, customer phone numbers, customer's smartphones, social media, discount campaigns, and data science analysis of which product and how much customers consume. However, it is seen that new technological applications that have become widespread in the retail sector generally focus on the customer and the product. In the scope of this study, innovative solutions for store employee, which is another pillar of the sector, are included. By using the proposed innovative hybrid solution, it is targeted that the store sales team will work more efficiently and effectively, thus improving the loyalty of the customers to the store and their shopping continuity, and ultimately improving the productivity of the store.

To determine whether the customers visiting the store receive the attention they expect regarding the products they are interested in, quickly and appropriately from the store employees a long with to increase the satisfaction of the customers regarding the services they receive from the store employees, a Virtual Merchandisor (vMerch)-Team" has been developing.

The vMerch-Team solution provides real-time tracking of store employees with indoor positioning technologies. Thus, the behaviors and activities of employees, both individually and as a team, can be monitored in the store. The performances of store employees are evaluated with data sets obtained as a result of monitoring over business intelligence approaches.

In summary, vMerch-Team is a solution that automatically performs the tasks of tracking store employees based on location and time. These include finding/capturing store employees,

identifying and tracking employees, taking action based on customer density in store, and creating analytics such as location analytics, behavior analytics.

Indoor ecosystem in retail

Indoor Positioning System generally includes technologies and positioning methods used to determine the location of a receiver in an indoor environment. Today, however, the concept of the indoor ecosystem has expanded substantially and has evolved from indoor location determination to indoor navigation, location-based services, context-aware services and reasoning.

In indoor positioning systems and Location-Based Service applications, roughly, the location of a user is determined using generally wireless radio technology and path planning is executed for the user to reach the place of interest. In the retail sector, however, it is generally desired to follow the customer density or product in the store through indoor localization applications. Proximity Marketing can be given as an example of the prominent indoor application in the retail industry. While employee tracking is carried out with GNSS receivers in the open area, electronic personnel cards are used in enclosed environments. Such an approach through the cards produces only general information in accordance with the Personnel Attendance Control System requirements, such as the hours in which the employee is in the store and the entry-exit hours.

Although there is a wide variety of approaches using different technologies and methods in IPS domain, Radio Frequency (RF) based technology seems to be more common in practice than others. On the other hand, the rapid development of computer vision, video processing, and deep learning makes image-based localization one of the fastest-growing indoor positioning and tracking techniques.

The proposed solution: "vMerch"

In this study, Indoor Positioning was designed as a hybrid solution. Firstly, the positioning technique with wireless radio waves, in which the user interacts with the wireless sensor network via wearable devices, and secondly, the image-based positioning technique, in which the user does not interact with the system, was developed separately. Although the first technique using radio signal power and the second technique using optical image are different from each other, they are used together to produce location information. The reason why an approach in which data sets obtained from different sources in different structures is used together is preferred within the scope of the study is that both techniques have pros and cons. Thus, the solution, in which two different techniques are used in a way that supports each other, will ensure that the system works continuously with high performance and will produce reliable outputs for other systems and analyzes to be made.

Stores are cluttered and crowded environments. Additionally, crowded customers around the products may prevent the store employee from being viewed by the camera or performing the correct face recognition from the image. In these and similar cases, information about where and how long the store employee has been can be produced by wireless radio technology. On the contrary, the store employee can give his radio signal tag to another employee. In this case, this employee will be followed by being matched with a different identity. Such situations can also be avoided by using image-based systems.

The main problem to be solved in the hybrid approach proposed in the study is how to use two different techniques with different structures in an integrated manner.

Positioning approach with RF techniques is performed by signal strength and is based on RSSI value. By applying classification algorithms to RSSI values, the location information is given generally on the fingerprint map (RF-map).

In image-based technique, stereo image and depth map can be produced from RGB-D source images or using more than one camera. If a single camera is used, location information can be produced by the help of the grids pre-generated on the image.

Apart from these two spatial representations, there is also a basic map (indoor map, metric map) that reflects the geometric representation of the environment.

In this case, the solution of the problem evolves from sensor fusion to map fusion (map matching). The map fusion

In this study, Indoor Positioning was designed as a hybrid solution. Firstly, the positioning technique with wireless radio waves, in which the user interacts with the wireless sensor network via wearable devices, and secondly, the image-based positioning technique, in which the user does not interact with the system, was developed separately.

Thematic maps like heat maps produced on the subjects, such as what products the customers are particularly interested in in the store, how long the customers stay in which part of the store, or how much time they spend in which product group, were also included in the map fusion.

problem can be solved by transformation. The coordinate system from which the base map was produced should be taken as the base coordinate system and other spatial representations such as fingerprint maps should be integrated in the base coordinate system. Thus, the locations and traces of movements of employees can be visualized on the base map.

Thematic maps like heat maps produced on the subjects, such as what products the customers are particularly interested in in the store, how long the customers stay in which part of the store, or how much time they spend in which product group, were also included in the map fusion.

In summary, the map engine being developed within the scope of vMerch-Team can spatially integrate the base map with topological features and other maps such as fingerprint, grid display and thematic maps. The interface being developed also visualizes the map and map information according to the roles and rights of the user.

References

Benezeth, Y., Emile, B., Laurent, H., "Vision-Based System for Human Detection and Tracking in Indoor Environment", Int J of Soc Robotics (2010) 2: 41. https://doi.org/10.1007/s12369-009-0040-4

Duque Domingo J, Cerrada C, Valero E, Cerrada JA. An Improved Indoor Positioning System Using RGB-D Cameras and Wireless Networks for Use in Complex Environments. Sensors (Basel, Switzerland). 2017;17(10):2391. doi:10.3390/s17102391.

George Galanakis, Xenophon Zabulis, Panagiotis Koutlemanis, Spiros Paparoulis, and Vassilis Kouroumalis. 2014. Tracking persons using a network of RGBD cameras. In Proceedings of the 7th International Conference on PErvasive Technologies Related to Assistive Environments (PETRA '14). ACM, New York, NY, USA, Article 63, 4 pages. DOI: https://doi.org/10.1145/2674396.2674467

Jaime Duque Domingo, Carlos Cerrada, Enrique Valero, and J. A. Cerrada, "Indoor Positioning System Using Depth Maps and Wireless Networks," Journal of Sensors, vol. 2016, Article ID 2107872, 8 pages, 2016. doi:10.1155/2016/2107872

Leykin, A., 2007, "Visual Human Tracking And Group Activity Analysis: A Video Mining System For Retail Marketing", Doctor of Philosophy, in Computer Science and Cognitive Science, Indiana University, December 2007

Luo, Wenhan & Xing, Junliang & Milan, Anton & Zhang, Xiaoqing & Liu, Wei & Zhao, Xiaowei & Kim, Tae-Kyun. (2017). Multiple Object Tracking: A Literature Review.

Massimo Camplani, Adeline Paiement, Majid Mirmehdi, Dima Damen, Sion Hannuna, Tilo Burghardt, Lili Tao, "Multiple human tracking in RGB-depth data: a survey," in IET Computer Vision, vol. 11, no. 4, pp. 265-285, 6 2017. (UK-Bristol)

Paul, M., Haque, S.M.E. & Chakraborty, S., 2013, "Human detection in surveillance videos and its applications - a review," EURASIP Journal on Advances in Signal Processing. (2013) 2013: 176. https://doi.org/10.1186/1687-6180-2013-176

Yilmaz, A., Javed, O., and Shah, M., 2006, "Object Tracking: A Survey", Journal of ACM Computing Surveys (CSUR) Surveys Homepage archive, Volume 38 Issue 4, 2006, Article No. 13, ACM New York, NY, USA. (December 2006). DOI=http://dx.doi.org/10.1145/1177352.1177355

Y. Wang, K. Lu and R. Zhai, "Challenge of multi-camera tracking (Technique and Challange for Multi-Camera Tracking)," 2014 7th International Congress on Image and Signal Processing, Dalian, 2014, pp. 32-37.

R. Mautz and S. Tilch, "Survey of optical indoor positioning systems," 2011 International Conference on Indoor Positioning and Indoor Navigation, Guimaraes, 2011, pp. 1-7.

E. Trucco and K. Plakas, "Video Tracking: A Concise Survey," in IEEE Journal of Oceanic Engineering, vol. 31, no. 2, pp. 520-529, April 2006.

The paper originally published in the proceedings of the 16th International Conference on Location Based Services is republished with authors' permission.

Performance assessment of GNSS-based real-time navigation for the Sentinel-6 spacecraft

GNSS-based onboard orbit determination can now reach a similar performance as the DORIS (Doppler Orbitography and Radiopositioning Integrated by Satellite) navigation system. It lends itself as a viable alternative for future remote sensing missions

Oliver Montenbruck
Deutsches Zentrum für Luft- und Raumfahrt (DLR), German Space Operations Center, 82234 Wessling, Germany

Florian Kunzi
Deutsches Zentrum für Luft- und Raumfahrt (DLR), German Space Operations Center, 82234 Wessling, Germany

André Hauschild
Deutsches Zentrum für Luft- und Raumfahrt (DLR), German Space Operations Center, 82234 Wessling, Germany

Abstract

The feasibility of precise real-time orbit determination of low earth orbit satellites using onboard GNSS observations is assessed using six months of flight data from the Sentinel-6A mission. Based on offline processing of dual-constellation pseudorange and carrier phase measurements as well as broadcast ephemerides in a sequential filter with a reduced dynamic force model, navigation solutions with a representative position error of 10 cm (3D RMS) are achieved. The overall performance is largely enabled by the superior quality of the Galileo broadcast ephemerides, which exhibits a two- to three-times smaller signal-in-space-range error than GPS and allows for geodetic grade GNSS real-time orbit determination without a need for external correction services. Compared to GPS only processing, a roughly two times better navigation accuracy is achieved in a Galileo only or mixed GPS/Galileo processing. On the other hand, GPS tracking offers a useful complement and additional robustness in view of a still incomplete Galileo constellation. Furthermore, it provides improved autonomy of the navigation process through the availability of earth orientation parameters in the new civil navigation message of the L2C signal. Overall, GNSS based onboard orbit determination can now reach a similar performance as the DORIS (Doppler Orbitography and Radiopositioning Integrated by Satellite) navigation system. It lends itself as a viable alternative for future remote sensing missions.

Introduction

Sentinel-6A "Michael Freilich," also known as Jason Continuity of Service (Jason-CS), is the latest satellite of the European earth observation program (Donlon et al. 2021). The primary payload comprises the Poseidon-4 Ku/C-band altimeter and the advanced microwave radiometer climate quality (AMR-C). Altimeter processing relies on highly accurate knowledge of the orbital position of the spacecraft, specifically its altitude, to determine the mean height of the sea level. Sentinel-6A precise orbit determination (POD) is supported by two independent sensors, namely a Doppler Orbitography and Radiopositioning Integrated by Satellite (DORIS) receiver (Auriol and Tourain 2010) and a "PODRIX" dual constellation global navigation satellite system (GNSS) receiver. For utmost accuracy, data from these instruments are processed on the ground in non-time critical (NTC) or short-time critical (STC) processes. In addition, the DORIS Immediate Orbit DEtermination (DIODE; Jayles et al. 2010) system provides onboard navigation solutions with roughly 10 cm (3D RMS) position accuracy and 2–3 cm height accuracy based on real-time

processing of Doppler measurements from a network of globally distributed ground beacons. External calibration and validation of orbit products are supported by a laser retroreflector for satellite laser ranging (SLR).

The PODRIX receiver likewise provides a real-time onboard navigation solution, which is mainly intended for platform support rather than science data processing and confined to an accuracy of roughly 3 m. The achieved performance reflects a trade off between performance, algorithmic complexity, and robustness and reflects typical accuracy needs for attitude and orbit control systems of LEO satellites.

It is largely determined by the use of GNSS broadcast ephemerides and basic dynamical models for Kalman filtering, as well as the sole use of GNSS pseudorange measurements. Notably higher accuracy can, in principle, be achieved by processing GNSS carrier phase observations as shown in past research and flight demonstrations of GNSS-based real-time orbit determination for satellites in low earth orbit (LEO). Montenbruck and Ramos-Bosch (2008) presented a reduced dynamics navigation filter for LEO satellites and achieved accuracies of 0.5–0.7 m 3D RMS based on playblack processing of actual dual-frequency GPS observations from five LEO missions in the 400–800 km altitude range. Onboard the PROBA-2 spacecraft, a 1.1 m 3D RMS accuracy was demonstrated with the eXtended Navigation System (XNS) of the Phoenix single-frequency GPS receiver, which could further be improved to 0.7 m in a reprocessing on ground with optimized filter settings (Montenbruck et al. 2012). More recently, Wang et al. (2015), Gong et al. (2019), and Gong et al. (2020) assessed the performance of similar real-time navigation algorithms through offline processing of GPS or GPS/BeiDou-2 measurements from various spacecraft of the USA, Europe, and China. Here 3D position errors of 0.4–0.7 m were obtained based on single- and dual-frequency observations, respectively.

In all of the above analyses, the achievable accuracy of GNSS-based real-time navigation is ultimately limited by the accuracy of GNSS broadcast ephemerides. For GPS, signal-in-space range errors (SISRE) have gradually decreased from roughly 1 m to 0.5 m over the past decade, which contributes to the continued improvement seen over time in the aforementioned studies. Even though the use of process noise in the carrier phase ambiguity states of the navigation filter (Montenbruck and Ramos-Bosch 2008; Wang et al. 2015) can, to a notable extent, reduce the impact of slowly varying GPS orbit and clock offset errors, a 1-dm LEO navigation accuracy appears out of reach today when relying only on GPS navigation data without augmentation. The use of real-time correction data has therefore been suggested by multiple authors (Reichert et al. 2002; Toral et al. 2006; Hauschild 2016; Giordano et al. 2017; Kim and Kim 2018; Murata et al. 2020), but the practical application of this concept is hampered by the limited availability of suitable modems or GNSS receivers for acquiring such correction data on LEO platforms.

With the ongoing build-up of the Galileo constellation, prospects for GNSS-based onboard navigation of LEO satellites have greatly improved in view of its remarkably accurate broadcast ephemerides. At SISRE values of 0.1–0.2 m (Montenbruck et al. 2018), Galileo clearly outperforms GPS and other GNSSs and reduces the contribution of broadcast ephemeris errors in the observation model to less than a wavelength. Carrier-phase-based positioning techniques, which have previously been limited to use with precise ephemerides or augmentation services, can now successfully be applied with orbit and clock data from the standard navigation messages (Carlin et al. 2021). These advantages are likewise of interest for GNSS-based onboard navigation of LEO satellites, which largely relies on the use of un-augmented broadcast ephemerides. Notable benefits of Galileo for this application have been earlier predicted in a simulation study of Hauschild and Montenbruck (2021) but lack a practical confirmation so far. Using actual flight data from the Sentinel-6A satellite now allows to reliably demonstrate the feasibility of 1 dm (3D RMS) real-time navigation using joint GPS and Galileo observations and shows that GNSS offers a viable alternative to DORIS for real-time orbit determination of LEO satellites.

Following a presentation of the GNSS data collected by the PODRIX receiver onboard of Sentinel-6A and relevant auxiliary data, we discuss the real-time navigation algorithms and model trade-off for the present study. Thereafter, real-time navigation results obtained in post processing from half a year of flight data are presented and the achieved performance is assessed. Furthermore, results are compared against actual real-time navigation results from the DORIS/DIODE system onboard Sentinel-6A and comparable performance of GPS/Galileo-based navigation is demonstrated.

Data

The present study covers a six month period from mid December 2020 to mid June 2021 after initial orbit acquisition of the Sentinel-6A spacecraft. It is based on GNSS observations of the PODRIX GNSS receiver and measured attitude information provided as part of the platform and science telemetry. Complementary spacecraft related information includes the mass and GNSS antenna phase center offset from the center-of-mass, as well as information on the time, duration, and planned velocity increment of orbit keeping maneuvers conducted on four days (Feb. 18, Apr. 27/29/30) within the analysis period. Even though the telemetry interface of the PODRIX receiver allows for transmission of a comprehensive set of GPS LNAV and CNAV (IS-GPS-200 2021) as well Galileo INAV and FNAV (EU 2021) broadcast ephemeris parameters, not all of the respective PODRIX output messages are enabled on the Sentinel-6A satellite. To overcome this limitation, which mainly affects the availability of group delays and earth orientation parameters (EOPs), broadcast

ephemeris data collected by a global receiver network and made available in the draft RINEX 4 navigation data format (Romero 2021) are used instead for the present study. Other than its predecessors, RINEX 4 provides full support of modernized navigation messages such as the CNAV message of the GPS L2C and L5 signal as well as system time offsets, ionosphere data, and EOPs.

While the ground collected navigation data cover all data transmitted by all GNSS satellites on a day of interest, they are fully representative of the GPS/Galileo orbit, clock offset, group delay, and EOP data available onboard for those GNSS satellites actually tracked by the PODRIX receiver. As such, they provide a legitimate substitute for missing telemetry data in our playback real-time navigation filter.

Concerning observations, the PODRIX receiver does not, by itself, provide a full set of pseudorange and carrier phase observations but rather outputs the code phase, i.e., the transmit time of the ranging signal and the phase of the numerically controlled oscillator that compensates the nominal intermediate frequency and Doppler shift of the down converted signal. Based on these data, conventional pseudorange and carrier phase observations can be formed with knowledge of the receiver time at the instant of the measurement (Won and Pany 2017). For the present work, a receiver time scale aligned to roughly 10 ns with the GPS time scale based on the receiver internal navigation solution is used. The resulting observations are stored on a daily basis in RINEX observation files with 10 s sampling for the subsequent processing.

In the default configuration used on Sentinel-6A, the PODRIX receiver uses a semi codeless tracking of the P(Y) signal on the L1 and L2 frequency for GPS Block IIR satellites, while the civil L2C signals are tracked for IIR-M, IIF, and GPS III satellites. In addition, the L1 C/A code signal is tracked for all GPS satellites. For Galileo satellites, the E1 Open Service pilot signal and the E5a pilot signal are tracked. The respective observations and tracking modes are identified by their RINEX identifiers (1W/2W, 1C/2L, 1C/5Q) within this work. In the period of interest, daily averages of 1.8 GPS IIR satellites, 6.0 GPS IIR-M/IIF/III satellites, and 6.3 Galileo satellites were typically tracked at the adopted 10° elevation mask (Fig. 1). For completeness, it is noted that the two Galileo satellites in eccentric orbits (identified as E14 and E18) are not tracked by the PODRIX receiver on Sentinel-6A, since they are not included in the Galileo almanac. Root-mean-square (RMS) pseudorange errors of the ionosphere-free dual-frequency combinations amount to roughly 0.5–0.7 m for GPS 1W/2W and 1C/2L observations and 0.3–0.4 m for Galileo 1C/5Q.

For illustrating the quality of the broadcast ephemeris data, the orbit, clock, and signal-in-space range errors (Montenbruck et al. 2018) for dual-frequency processing are summarized in Table 1 for a sample month in the data analysis period. In case of GPS, separate values are provided for the use of LNAV messages with legacy P(Y) signals as well as CNAV messages with the civil L1 C/A and L2C signals. Differences between the two cases relate to the use of different Keplerian orbit models for fitting the predicted ephemeris as well as the quality of group delay parameters for mapping the clock offset parameters to the observed signals when using the civil L1 C/A and L2C signals. Compared to GPS with roughly daily ephemeris uploads, Galileo benefits primarily from an ephemeris refresh rate of mostly 10 – 30 min and achieves an up to four times smaller SISRE of down to 10 cm.

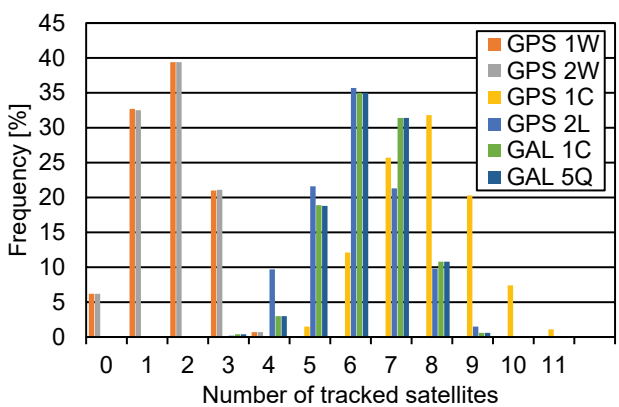

Fig. 1 Distribution of the number of satellites tracking individual signals

Algorithms and models

The "RTNAV" navigation filter software used for the processing of Sentinel-6A GNSS data is described in this section with focus on dynamical and observations models as well as parameter adjustment. The algorithms build on previous work reported in Montenbruck and Ramos-Bosch (2008) but differ in selected aspects such as the choice of the reference system and specific force model contributions, as well as the multi-signal, multi-GNSS extension. While the actual data processing for the present study was performed on a desktop computer in a simulated real-time mode, the core algorithms have earlier been demonstrated in flight (Montenbruck et al. 2012) and are thus considered compatible with the limited resources of representative onboard computers. A summary of various processing models is given in Table 2, which also lists the corresponding counterpart of the DIODE

Table 1 Orbit, clock, and signal-in-space range errors [RMS, in (m)] for May 2021

	GPSLNAV LI/L2 P(Y)	GPSCNAV L1CA/L2C	GALFNAV EI/E5a
Radial	0.15	0.14	0.13
Along-track	1.02	0.97	0.28
Cross-track	0.38	0.39	0.19
Clock	0.36	0.38	0.16
SISRE (orbit)	0.21	0.20	0.14
SISRE	0.41	0.43	0.10

real-time navigation software for onboard processing of DORIS observations (Auriol and Tourain 2010; Jayles et al. 2016).

Trajectory model

The algorithm builds on a reduced-dynamic (Yunck et al. 1994) trajectory model for propagating the satellite orbit between consecutive measurement updates in an extended Kalman filter. Here, an a priori set of physical models for the spacecraft motion is complemented by empirical accelerations that are adjusted in the filter to compensate potential deficiencies of the a priori model. While gravitational forces can be modeled with good confidence, limitations typically apply for non-gravitational forces that would require detailed knowledge of the spacecraft structure and surface parameters. For Sentinel-6A, which orbits the earth at an altitude of roughly 1340 km, a 50 × 50 subset of the GGM01S gravity model (Tapley et al. (2004b)) is adopted and tidal variations are approximated by a basic k2 solid earth tide model (Rizos and Stolz 1985). For an efficient and numerically stable evaluation of the acceleration from the geopotential coefficients, the formulation of Cunningham (1970) is used. Luni-solar perturbations are described through a point-mass model using approximate analytical models of the sun and moon position with representative accuracies of 1 to 5 arcminutes (Montenbruck and Gill 2000).

Drag, which has an almost negligible impact at the orbital height of Sentinel-6A, is described through a cannon-ball model with a static Harries and Priester (1962) density model and an adjustable scale factor (C_D). For solar radiation pressure (SRP), a cannon-ball model with an adjustable scale factor (C_R) is applied along with a cylindrical shadow model. Earth-radiation pressure (ERP) is approximated by a constant radial

Table 2 Processing models for Sentinel-6A real-time orbit determination

RTNAV	DORIS
Trajectory mo el	
Reference system: celestial	Celestial
Gravitational forces: GGM01S earth gravity field model (50×50), k_2 tides, point-mass model for sun and moon with simplified analytical ephemeris	EIGEN 6S (up to 78×78), luni-solar perturbations with Meeus sun/moon position models, relativistic acceleration
Surface forces: cannon-ball model for solar radiation pressure and atmospheric drag, static Harris-Priester density model, radial acceleration for earth radiation pressure	Solar radiation pressure (macro model), albedo and infrared earth radiation pressure (Knocke–Ries model)
Others: constant thrust arcs (maneuvers); empirical accelerations in radial, along-track and cross-track direction	Thrust, orbit-periodic cross-tack acceleration
Numerical integration: DOPRI5 Runge–Kutta method, 30 s step size, 4th-order interpolant	4th-order Runge–Kutta–Gill
Observation mo el	
Observations: Undifferenced ionosphere-free code and carrier phase combination (L1 C/A and L2C or L1/L2 P(Y) for GPS, E1 and E5a pilot for Galileo)	DORIS phase-difference measurements, ionosphere-free dual-frequency combination (S-Band, UHF)
GNSS orbits and clock offsets: broadcast ephemerides (GPS LNAV, Galileo FNAV)	Fixed beacon coordinates
	Atmospheric correction: troposphere (mapping function and estimated bias)
Group delays: TGD and ISC for L1 C/A and L2C from GPS CNAV message	
GNSS antenna: zero phase center offset, no patterns (not applicable for use with broadcast ephemerides)	
Receiver antenna: phase center offset from inflight calibration (75 mm/93 mm for GPS/GAL), no phase patterns	
Carrier phase wind-up: modeled	
Reference frame: celestial-to-earth-fixed transformation based on IERS1996 conventions and GPS CNAV earth orientation parameters, no sub-daily tides	Estimated pole coordinates
Attitude: quaternions	Quaternions
Estimation	
Extended Kalman filter with vector measurement update	Separate Kalman filters for orbit and clock, UD formulation
60 s update interval	10 s update interval
Estimated parameters: position/velocity, force model scale factors, empirical or thrust accelerations, clock offset, inter-system bias, carrier phase ambiguities	Estimated parameters: position/velocity, 1/rev along- and cross-track acceleration, thrust, drag scale factor, pole coordinates, beacon and receiver clock frequency bias and drift, troposphere bias

acceleration with a value of 30 nm/s^2 that represents the average acceleration obtained from more detailed ERP models for the Sentinel-6A spacecraft and orbit (Montenbruck et al. 2021). Finally, piecewise constant accelerations in radial (R), along-track (T), and cross-track (N) direction can be applied to describe empirical accelerations or thrust arcs during orbit control maneuvers. Such maneuvers are modeled using a priori information on the start time, duration, and approximate velocity increment in the three axes. Within the Kalman filer, additional process noise in the position and velocity states is used to compensate errors in the a priori maneuver modeling.

The equation of motion is formulated as a first-order differential equation

$$\begin{pmatrix} \dot{\boldsymbol{r}} \\ \dot{\boldsymbol{v}} \end{pmatrix} = \begin{pmatrix} \boldsymbol{v} \\ \boldsymbol{a}(t, \boldsymbol{r}, \boldsymbol{v}) \end{pmatrix} \quad (1)$$

for the position $\boldsymbol{r}$ and velocity $\boldsymbol{v}$ as a function of the time t and the acceleration $\boldsymbol{a}$. Contrary to Montenbruck and Ramos-Bosch (2008), who proposed an earth-fixed formulation of the equation of motion to minimize the need for reference system transformations, an inertial formulation is adopted in the present work. It implies the need for explicit transformations between the celestial and terrestrial reference systems in the observation model and on the output of the estimated state vector. Despite a higher computational effort, the inertial formulation is preferred here to avoid the impact of small simplifications in the modeling of Coriolis forces in the earth-fixed approach. These simplifications were found to require larger empirical accelerations, particularly in the cross-track direction, and ultimately limit the achievable orbit determination accuracy.

Next to the equation of motion, a simplified set of variational equations is used to establish the state-transition matrix and the position/velocity partials with respect to SRP and drag scale factors as well as the RTN accelerations. The six-stage, fifth-order Runge–Kutta method of Dormand and Prince (1980) is used for numerical integration of the equation of motion and the variational equations with a fixed step-size of 30 s. The method can be favorably combined with a fourth-order interpolant (Hairer et al. 1987) to support dense output. This allows the generation of trajectory information at, e.g., 1 s or 10 s, without limiting the actual integrator step size.

Observation model

In accord with the capabilities of the PODRIX receiver on Sentinel-6A, the RTNAV filter is designed to support GNSS observations of satellite-specific signals and from multiple constellations. The ionosphere-free pseudorange (p) and carrier-phase (φ) observations are thus described by the generic observation model

$$\begin{aligned} p &= |\boldsymbol{r}^k - \boldsymbol{r}| + c\left(\mathrm{d}t_{\mathrm{rcv}} + \mathrm{d}t^{c_k} - \mathrm{d}t^k\right) + B^{k,s_k,s_{\mathrm{ref},k}} \\ \varphi &= |\boldsymbol{r}^k - \boldsymbol{r}| + c\left(\mathrm{d}t_{\mathrm{rcv}} + \mathrm{d}t^{c_k} - \mathrm{d}t^k\right) + A^k + \Psi^k \end{aligned} \quad (2)$$

where $|\boldsymbol{r}^k - \boldsymbol{r}|$ denotes the distance between the position r^k of a tracked satellite k of constellation c_k at signal transmission and the receiver r at signal reception. $\mathrm{d}t^k$ denotes the satellite clock offset relative to the constellation-specific system time as provided in the broadcast navigation message. Analogously, $\mathrm{d}t_{\mathrm{rcv}}$ denotes the receiver clock offset. It is referred to a selected reference constellation, here GPS, and the corresponding reference signal of the broadcast clock offsets, i.e., the ionosphere-free combination of L1 and L2 P(Y)-code observations. The inter-system bias, or ISB, $\mathrm{d}t^{\mathrm{ck}}$ is conventionally set to zero for the reference constellation. For satellites of other constellations, it combines the system time difference, here the Galileo-GPS time offset (GGTO), and receiver and constellation-specific biases between the tracked signals and the reference signals. Despite an a priori calibration of receiver biases in the PODRIX receiver data, residual biases cannot be neglected in practice and must be adjusted in the orbit and clock determination. As such, they can readily be lumped with the GGTO and no need arises to explicitly use the GGTO value provided in the Galileo navigation message.

For pseudorange measurements, the observation model furthermore accounts for a satellite code bias contribution $B^{k,s_k,s_{\mathrm{ref},k}}$, which depends on the satellite k, the tracked set of signals s_k and the set of broadcast clock reference signals $s_{\mathrm{ref},k}$ for the specific constellation. In the present application, the bias vanishes for GPS P(Y) tracking as well as Galileo E1/E5a tracking in combination with the use of FNAV ephemerides. For GPS L1 C/A and L2C tracking in contrast, the bias does not vanish and needs to be applied in the model. It is formed from the timing group delay parameter, TGD, and the $\mathrm{ISC}_{\mathrm{L2C}}$ inter-signal correction as detailed in IS-GPS-200 or Montenbruck and Hauschild (2013). For carrier-phase observations, an ambiguity term A^k is included in the observation model. It is adjusted from the observations and lumps any remaining carrier phase biases that are not explicitly considered in the model. Furthermore, it is used to absorb errors on the modeled carrier phase caused by broadcast orbit and clock errors by allowing for process noise in the estimation of these parameters. Following Wu et al. (1993), the carrier phase model also considers the contribution of phase wind-up Ψ based on the time-varying orientation of the transmit and receive antennas.

The observation model is evaluated with satellite and receiver positions in an earth-fixed reference frame that aligns with the reference frame of the broadcast ephemerides. While GPS and Galileo make use of constellation-specific realizations of the international terrestrial reference system, namely WGS84 and GTRF, differences with respect to each other and the most recent version of the international reference frame, ITRF2014, are at the centimeter level (NGA 2021; Enderle 2018; Malys et al. 2021) and have been neglected in the present context. Following the numerical integration of the equation of motion, the spacecraft position needs to be transformed from the celestial to the terrestrial frame to obtain the ITRF position of the receiver antenna as required by the observation model. The IERS 1996 models (McCarthy 1996) of precession, nutation, and earth rotation

are adopted for this purpose in view of a reduced complexity compared to the more rigorous IERS 2010 conventions (Petit and Luzum 2010). For improved efficiency, trigonometric functions in the nutation model are recursively computed using addition theorems. Pole coordinates x_p and y_p as well as the UT1-UTC difference required in the transformation at the epoch of interest are obtained from predictions of these values transmitted in the form of linear polynomial approximations within the CNAV navigation message of the GPS L2C signal and updated once per day by the ground segment.

For completeness, we note that the observation model ties the estimated spacecraft position to the earth fixed frame that is implied by the broadcast ephemerides of the tracked GNSS satellites. Uncertainties or approximations in the celestial-to-terrestrial transformation mainly affect the realization of the inertial system used for the trajectory propagation, which may thus deviate slightly from the International Celestial Reference System (ICRF). However, the transformation from this approximate celestial system using the approximate ICRF-to-ITRF transformation correctly replicates the observed motion in the WGS84/GTRF frame. As such, only the earth fixed position and velocity output by the navigation filter will be used for comparison with reference orbit products to assess the achievable real-time navigation accuracy.

Estimation

An extended Kalman filter is used to adjust the position, velocity and receiver clock at the time of the measurement. Overall, the filter state

$$\boldsymbol{Y} = (\boldsymbol{r}^{\mathrm{T}}, \boldsymbol{v}^{\mathrm{T}}, C_R, C_D, a_R, a_T, a_N, \mathrm{d}t_{rcv}, \mathrm{d}t^{\mathrm{GAL}}, A_1, \ldots, A_n)^{\mathrm{T}}$$

comprises the inertial position and velocity of the spacecraft center-of-mass, the SRP and drag scale factors (C_R, C_D), empirical accelerations or thrust accelerations (a_R, a_T , a_N) in radial, along-track and cross-track direction, the GPS-referenced receiver clock offset, the ISB for Galileo, and a carrier phase ambiguity for each of the tracked satellites. In the time update step of the filter, position and velocity are propagated through numerical integration, while the force model scale factors, clock parameters, and ambiguities are predicted with a unit state transition matrix. Empirical accelerations are treated as exponentially correlated random variables (Tapley et al. 2004a). They are kept constant during the numerical trajectory propagation from the last epoch t_{i-1} to the new measurement epoch $t_i = t_{i-1} + \Delta t$, but their predicted value at that epoch is obtained by scaling with an exponential damping factor $m = e^{\Delta t/\tau}$ using a predefined correlation time τ with a representative value of 600 s. White process noise with variance q proportional to the measurement interval is applied to the **SRP** and drag scale factors as well as the clock and **ISB** states, while the process noise variance

$$q = \sigma_a^2 (1 - m^2)$$

of the empirical accelerations depends on the selected steady state variance σ_a and the exponential mapping factor.

GNSS carrier phase ambiguities are conceptually constant values and no process noise would normally be applied in their estimation. However, as previously discussed in Montenbruck and Ramos-Bosch (2008) and Wang et al. (2015), process noise in the ambiguity states provides a convenient means to compensate the impact of signal-in-space range errors when working with broadcast ephemerides. Instead of adjusting a dedicated **SISRE** parameter for each tracked satellite that adds to both the modeled pseudorange and carrier phase (Gunning et al. 2019), gradually varying ephemeris errors can likewise be absorbed in a lumped state reflecting the sum of the ambiguity and **SISRE** parameter. While this approach ignores the **SISRE** contribution in the pseudorange, this simplification is generally acceptable in practice in view of the lower pseudorange weight and the comparatively short arcs of continuous carrier phase tracking for receivers onboard a **LEO** satellite. The amount of process noise applied in the ambiguity states is motivated by the constel-lation-specific variation in **GNSS** clock offsets errors and line-of-sight orbit errors. Process noise values minimizing the overall errors of the estimated trajectory can best be obtained with the filter tuning using a parametric search and a precise reference trajectory for the desired mission. In the present work, representative process noise variances of $q_A = (40\ \mathrm{mm})^2$ and $q_A = (14\ \mathrm{mm})^2$ were applied at measurement intervals of 60 s.

Results and discussion

Based on the algorithms and input data described above, GNSS navigation filter results for Sentinel-6A were computed in a simulated real-time mode. As a reference for the performance assessment and initial filter tuning, precise orbit determination results based on ambiguity-fixed processing of GPS and Galileo observations from the PODRIX receiver were used (Montenbruck et al. 2021). These reference orbits were independently verified through satellite laser ranging and show sub centimeter RMS residuals after consideration of station specific biases. Furthermore, they exhibit consistency better than 1 cm 3D RMS compared with the combined, multi agency solution generated as part of the Copernicus POD service (CPOD 2021).

Weekly solutions exhibit a stable performance with position errors of about 10 cm (Fig. 2). In each of these solutions, a 15-min interval at the beginning of the data arc has been excluded from the comparison to mask the early convergence phase of the navigation filter. The overall error budget is dominated by the along-track component, which is only weakly constrained by the dynamical models and exhibits errors of 6–8 cm RMS. Errors in the radial component, which are of primary relevance for altimetry, range from 3–4 cm RMS, while cross-track errors amount to 4–6 cm RMS. The combined error perpendicular to the flight direction is well within common

requirements for the generation of synthetic aperture radar (SAR) images (Roselló Guasch 2010; Breit et al. 2010), and a GNSS-based onboard navigation solution could thus facilitate quick look processing of SAR.

RMS velocity errors of the weekly solutions relative to the precise reference amount to 0.08–0.10 mm/s in the period of interest, and the along-track components of the velocity error are confined to 0.03–0.04 mm/s RMS. This falls well within the needs for (near-) real-time orbit determination of common radio occultation missions, which require a 0.05–0.20 mm/s along-track velocity accuracy to retrieve bending angle profiles from the observed Doppler excess (Kursinski et al. 1997, Roselló Guasch 2010). It must be noted, though, that the achievable accuracy of the velocity component depends largely on the quality of the a priori force model and clearly benefits from the comparatively high altitude of the Sentinel-6A mission. Spacecraft operated at lower altitudes and experiencing higher drag forces would typically require an increased level of empirical forces, which then reduces the dynamical constraints on the resulting orbit. Nevertheless, independent simulations of GNSS-based real-time navigation (Hauschild and Montenbruck 2021) suggest that a better than 0.1 mm/s along-track velocity accuracy can even be reached for spacecraft orbiting at down to 400 km altitude.

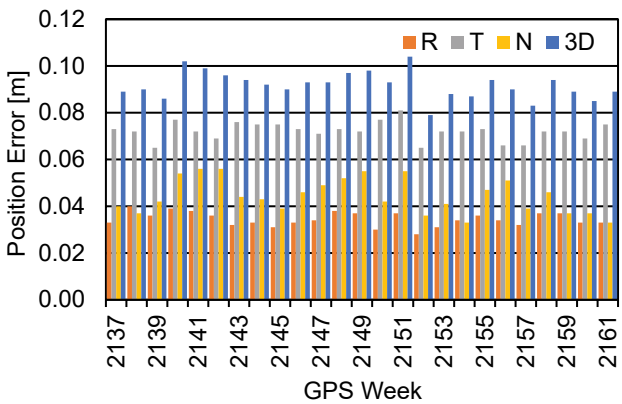

Fig. 2 RMS errors of the GNSS real-time navigation solutions in radial (R), along-track (T), and cross-track (N) direction as well as total position error (3D) relative to a precise orbit determination solu-tion from December 20, 2020 to June 12, 2021 (GPS week 2137–2161)

The achieved accuracy is clearly dominated by the contribution of Galileo, which offers both lower measurement noise and reduced broadcast ephemeris errors when compared to GPS. As shown in Table 3, a Galileo only processing can in fact provide an almost identical performance as the combined solution, while the stand-alone GPS solution shows roughly two times larger errors in all components. Given the reduced number of Galileo satellites available in the current mission phase and available for tracking by the PODRIX receiver, smaller errors may, however, be obtained on average in the start up phase of the navigation filter when jointly processing both constellations. Also, it must be emphasized that Galileo does not offer earth orientation parameters as part of its navigation messages and a regular EOP upload from the ground would therefore be required for LEO satellites using a Galileo only real-time navigation system.

As recognized from Table 3, the solutions of the GNSS navigation filter exhibit small but discernible mean offsets in the along-track and cross-track direction. In the latter case, the bias can, at least partly, be understood by an apparent inconsistency of about 7 mm in the center-of-mass offset of the GPS antenna provided by the manufacturer, which has previously been discussed in Montenbruck et al. (2021). While carrier phase ambiguity fixing aligns the precise orbit determination solution in such a way as to reflect the observed motion of the antenna properly, a float ambiguity processing tends to reflect the actual motion of the center of mass due to the dynamical constraints in orbit normal direction. Based on the analysis of satellite laser ranging measurements, a 7-mm cross-track bias has been identified in the POD solutions used as a reference for the present study, which can thus explain the dominant part of the mean cross-track bias of the GNSS real-time solutions. No indication of systematic offsets in the reference orbit exists for the along-track direction, and the biases in Table 3 must solely be attributed to the real-time navigation filter. Tests with different filter parameters show that the magnitude of the along-track bias depends on the amount of process noise applied in the ambiguity states and can be decreased at the expense of a higher overall position error. A mapping of along-track position errors into gradual variations in the carrier-phase ambiguities is therefore suspected as an explanation for the observed biases. However, given the magnitude of the along-track bias and its limited relevance in common applications of (near-)real-time orbit products, it appears well tolerable in practice.

As a final step of the performance characterization, we compare the solution of the GNSS navigation filter with the actual flight results of the DORIS/DIODE system on Sentinel-6A. The variation in position errors for a common 3-day interval is shown in Figs. 3 and 4 for the two techniques. In both cases, precise orbit determination results based on ambiguity-fixed GPS/Galileo observations from Montenbruck et al. (2021) were used as a reference for the performance analysis. Overall, both systems show an almost identical performance in radial and along-track direction, but a slightly different short-term behavior may be recognized for the latter. While the present results show a dominant once-per-revolution variation

Table 3 Errors of Sentinel-6A real-time navigation solutions using different sets of GNSS observations over the half-year analysis period

Constellations	Radial	Along-track	Cross-track	Position (RMS)
GPS	– 2 ± 61	– 7 ± 158	– 12 ± 107	200
Galileo	+ 1 ± 36	– 21 ± 71	– 9 ± 44	94
GPS+ Galileo	0 ± 35 –	17 ± 70	– 10 ± 44	92

For the individual axes, the mean value ± standard deviation of the errors are given. All values in mm

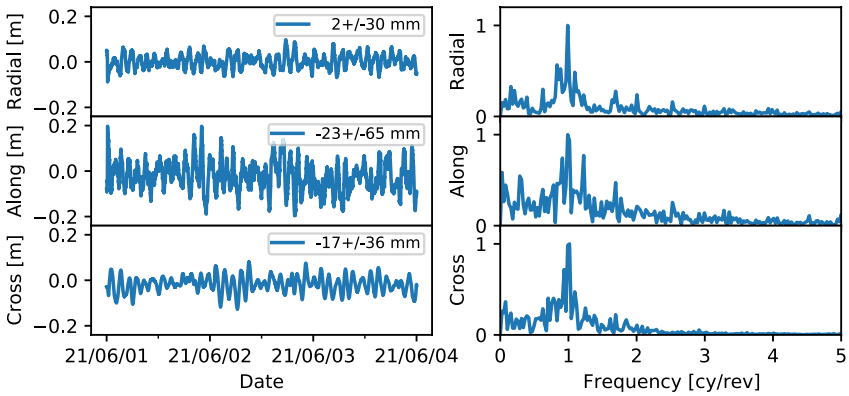

Fig. 3 Errors of the GNSS-based navigation filter in radial, along-track, and cross-track direction relative to a precise orbit determination solution for 1–3 June 2021 (left). Num-bers in the top right corner of each subplot denote the mean ± standard deviation of the respective errors. The right column shows the normalized frequency spectra of the posi-tion errors for the individual axes

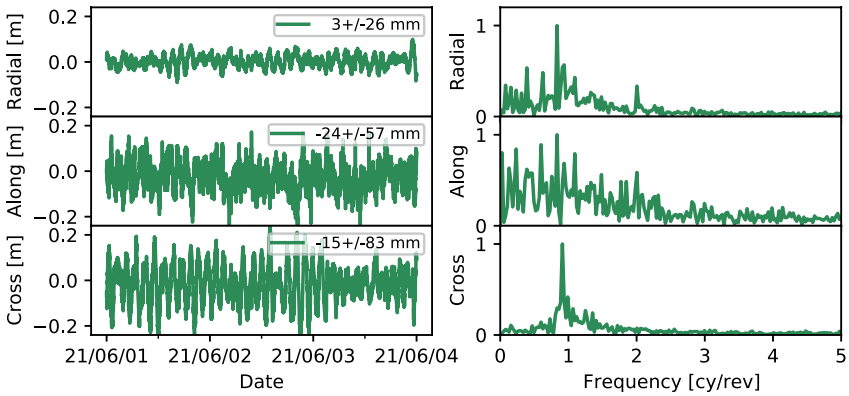

Fig. 4 Errors of the DORIS real-time navigation solution in radial, along-track, and cross-track direction relative to a precise orbit determina-tion solution for 1–3 June 2021 (left). Numbers in the top right corner of each subplot denote the mean ± standard deviation of the respective errors. The right column shows the normalized frequency spectra of the posi-tion errors for the individual axes

in the along-track-position error, the DIODE solution exhibits a slightly higher scatter on sub-orbital time scales. These differences indicate a higher reliance of the present GNSS navigation filter on the dynamical model for the current tuning, while the DIODE results are slightly more kinematic in nature and show a stronger influence of measurement noise. As the most obvious difference, larger errors in cross-track direction can be observed for the DIODE solution. These occur at a frequency of 0.92 cycles per orbital revolution, which differs from the orbital frequency (1 cy/rev) by the mean rate of earth rotation. Aside from a weaker geometric strength of the DORIS observations in cross-track direction, the performance difference may in part be attributed to differences in the empirical acceleration model. While DIODE applies a harmonic, once-per-revolution model, the cross-track acceleration is described by an exponentially correlated random variable in the GNSS navigation filter. Presumably, this model can compensate temporal variations in unmodeled accelerations in a better manner. For completeness, it is noted that further model improvements reducing the cross-track error to roughly 4–5 cm are available in a new DIODE software version, but have not yet been loaded on Sentinel-6A.

Summary and conclusions

The accuracy of GPS broadcast ephemerides has long limited GNSS-based real-time orbit determination of satellites in low earth orbit. These are characterized by signal-in-space range errors of roughly 0.5 m and have enabled 3D RMS positioning errors of the same magnitude in past studies of GPS-based real-time navigation. Notably, the Galileo system provides improved prospects for accurate onboard navigation of LEO satellites, which offers SISRE values of down to 0.1 m. Making use of actual flight data from the Sentinel-6A satellite, which hosts the first space-grade GPS/Galileo receiver, we assessed the achievable navigation accuracy with observations of both constellations.

The processing is performed with an extended Kalman filter that builds on a reduced dynamic force model and processes the pseudorange and carrier phase observations purely sequentially. For maximum accuracy, the impact of broadcast ephemeris errors is compensated by including a white noise parameter in the carrier phase observation model. This parameter lumps the actual phase ambiguity with GNSS clock and line-of-sight orbit errors, and ultimately enables a 0.1 m 3D RMS accuracy in the GPS + Galileo processing. A similar performance can, in principle, be achieved in Galileo only processing but requires external earth orientation parameters. These are presently only transmitted by the modernized GPS satellites and would need to be incorporated into the Galileo navigation message to enable fully autonomous Galileo only navigation of LEO satellites.

Overall, the achieved performance closely matches that of the DIODE system for DORIS-based real-time navigation onboard the Sentinel-6A satellite. So far, DIODE represents the only fully operational onboard navigation system that is able to achieve 10-cm real-time navigation for LEO satellites. The results achieved in the present study show that similar performance can now as well be achieved from GNSS observations. Nowadays, GNSS receivers for space applications are widely available, so GNSS-based real-time navigation systems can provide an interesting and complementary alternative to DORIS for

Making use of actual flight data from the Sentinel-6A satellite, which hosts the first space-grade GPS/Galileo receiver, we assessed the achievable navigation accuracy with observations of both constellations

state-of-the-art accuracy. Applications that can benefit from this development include science missions for altimetry, SAR imaging, or atmospheric profiling, but also satellite formations or mega constellations. In combination with commercial-of-the-shelf GNSS receivers, the technology is of particular interest for low-cost missions and missions with tight engineering budgets.

At a 10-cm 3D RMS position error, the GNSS-based real-time navigation solution is expected to meet even demanding needs for onboard position knowledge, but certainly still lags behind the performance achievable in ground-based POD. In part, this can be attributed to the forward only processing in sequential estimation schemes for real-time processing, which commonly shows a factor of two performance degradation compared to a forward–backward filter smoother or least squares estimator. As shown by the comparison of GPS and Galileo only processing, the broadcast ephemeris quality clearly impacts the achievable navigation performance. Use of real-time correction data could thus contribute to lower SISRE and a homogeneous quality for all tracked GNSSs, but the remarkable quality of Galileo broadcast ephemerides already sets a high standard for the performance of potential correction services. Furthermore, improved GNSS ephemeris data alone may not be sufficient, and further model improvements will likely be required when trying to bridge the performance gap between real-time and ground-based POD processing. This relates both to dynamical models, where improved a priori models for the nongravitational forces would reduce the need for empirical parameters, and measurement model improvements thus as use of phase pattern calibrations. Most notably, single-receiver ambiguity resolution would be expected to enable further improvements in the real-time orbit determination accuracy, but would require dedicated real-time GNSS orbit and clock products with associated code and phase bias information.

Acknowledgements

Sentinel-6A GNSS data used in this study have kindly been made available by EUMETSAT and the European Commission (EC) as part of the Copernicus program. The authors would also like to express their thanks to Centre National D'Etudes Spatiales (CNES) and Collecte Localisation Satellites (CLS) for the provision of DORIS/DIODE real-time navigation solutions, which served as a reference for the performance characterization of the present algorithms. Furthermore, we are grateful to the CNES/CLS DORIS team for valuable discussion on the DIODE system and their contribution to the review of this article.

Funding

Open Access funding enabled and organized by Projekt DEAL.

Open Access

This article is licensed under a Creative Commons Attribution 4.0 International License, which permits use, sharing, adaptation, distribution and reproduction in any medium or format, as long as you give appropriate credit to the original author(s) and the source, provide a link to the Creative Commons licence, and indicate if changes were made. The images or other third party material in this article are included in the article's Creative Commons licence, unless indicated otherwise in a credit line to the material. If material is not included in the article's Creative Commons licence and your intended use is not permitted by statutory regulation or exceeds the permitted use, you will need to obtain permission directly from the copyright holder. To view a copy of this licence, visit http:// creat iveco mmons. org/ licen ses/ by/4. 0/.

References

Auriol A, Tourain C (2010) DORIS system: the new age. Adv Space Res 46(12):1484–1496. https:// doi. org/ 10. 1016/j. asr. 2010. 05. 015

Breit H, Fritz T, Balss U, Lachaise M, Niedermeier A, Vonavka M (2010) TerraSAR-X SAR processing and products. IEEE Trans Geosci Remote Sens 48(2):727–740. https:// doi. org/ 10. 1109/ TGRS. 2009. 20354 97

Carlin L, Hauschild A, Montenbruck O (2021) Precise point positioning with GPS and Galileo broadcast ephemerides. GPS Solut 25(2):77. https:// doi. org/ 10. 1007/ s10291- 021- 01111-4

CPOD (2021) Copernicus POD Regular Service Review Apr.- Jun 2021, Copernicus Sentinel-1, -2, -3 and -6 Precise Orbit Determination Service (CPOD), GMV-CPOD-RSR-0021, 2021/06/23

Cunningham LE (1970) On the computation of the spherical harmonic terms needed during the numerical integration of the orbital motion of an artificial satellite. Celest Mech 2(2):207–216. https:// doi. org/ 10. 1007/ BF012 29495

Donlon CJ, Cullen R, Giulicchi L, Vuilleumier P, Francis CR, Kuschnerus M, Simpson W,

Bouridah A, Caleno M, Bertoni R et al (2021) The Copernicus Sentinel-6 mission: enhanced continuity of satellite sea level measurements from space. Remote Sens Environ 258:112395. https:// doi. org/ 10. 1016/j. rse. 2021. 112395

Dormand JR, Prince PJ (1980) A family of embedded RungeKutta formulae. J Comput Appl Math 6(1):19–26. https:// doi. org/ 10. 1016/ 0771- 050X(80) 90013-3

Enderle W (2018) Galileo Terrestrial Reference Frame (GTRF)— Status, ICG-13, 4–9 November 2018, Xi'an, China, UNOOSA. https:// www. unoosa. org/ docum ents/ pdf/ icg/ 2018/ icg13/ wgd/ wgd_06. pdf. Accessed 1 Aug 2021

EU (2021) European GNSS (Galileo) Open Service, Signal-in-Space, Interface Control Document, Issue 2.0

Giordano P, Zoccarato P, Otten M, Crisci M (2017) P2OD Realtime precise onboard orbit determination for LEO satellites In: Proceedings of ION GNSS+ 2017, Portland, Oregon, pp 1754–1771. https:// doi. org/ 10. 33012/ 2017. 15190

Gong X, Guo L, Wang F, Zhang W, Sang J, Ge M, Schuh H (2019) Precise onboard real-time orbit determination with a low-cost single-frequency GPS/BDS receiver. Remote Sens 11(11):1391. https:// doi. org/ 10. 3390/ rs111 11391

Gong X, Sang J, Wang F, Li X (2020) LEO onboard real time orbit determination using GPS/BDS data with an optimal stochastic model. Remote Sens 12(20):3458. https:// doi. org/ 10. 3390/ rs122 03458

Gunning K, Blanch J, Walter T (2019) SBAS corrections for PPP integrity with solution separation. In: Proceedings of ION ITM 2019, Reston, VA, USA, January 28–31, pp 707–719. https:// doi. org/ 10. 33012/ 2019. 16739

Hairer E, Norsett SP, Wanner G (1987) Solving ordinary differential equations I. Springer-Verlag, Berlin-Heidelberg-New York

Harris I, Priester W (1962) Time-dependent structure of the upper atmosphere. NASA 87-FM-2, Goddard Space Flight Center, MD

Hauschild A, Tegedor J, Montenbruck O, Visser H, Markgraf M (2016) Precise onboard orbit determination for LEO satellites with real-time orbit and clock corrections. In: Proceedings of ION GNSS+ 2016, Portland, Oregon, pp 3715–3723. https:// doi. org/10. 33012/ 2016. 14717

Hauschild A, Montenbruck O (2021) Precise real-time navigation of LEO satellites using GNSS broadcast ephemerides. NAVIGATION J Inst Navig 68(2):419–432. https:// doi. org/ 10. 1002/ navi.416

IS-GPS-200 (2021) NAVSTAR GPS Space Segment/Navigation User Interfaces, IS-GPS-200 Rev. M, 21 May 2021, Space and Missile Systems Center, Los Angeles Air Force Base

Jayles C, Chauveau JP, Rozo F (2010) DORIS/Jason-2: better than 10 cm onboard orbits available for near-real-time altimetry. Adv Space Res 46(12):1497–1512. https:// doi. org/ 10. 1016/j. asr. 2010. 04. 030

Jayles C, Chauveau JP, Didelot F, Auriol A, Tourain C (2016) DORIS system and integrity survey. Adv Space Res 58(12):2691–2706. https:// doi. org/ 10. 1016/j. asr. 2016. 05. 032

Kim J, Kim M (2018) Orbit determination of low-earth-orbiting satellites using space-based augmentation systems. J Spacecr Rocket 55(5):1300–1302. https:// doi. org/ 10. 2514/1. A34061

Kursinski ER, Hajj GA, Schofield JT, Linfield RP, Hardy KR (1997) Observing Earth's atmosphere with radio occultation measurements using the Global Positioning System. J Geophys Res 102(D19):23429–23465. https:// doi. org/ 10. 1029/ 97JD0 1569

Malys S, Solomon R, Drotar J, Kawakami T, Johnson T (2021) Compatibility of Terrestrial Reference Frames used in GNSS broadcast messages during an 8 week period of 2019. Adv Space Res 67(2):834–844. https:// doi. org/ 10. 1016/j. asr. 2020. 11. 029

McCarthy DD (1996) IERS Conventions (1996), IERS Technical Note No. 21, US Naval Observatory

Montenbruck O, Gill E (2000) Satellite orbits. Springer Verlag, Heidelberg

Montenbruck O, Hauschild A (2013) Code biases in multi-GNSS point positioning. In: Proceedings of ION ITM 2013, 28–30 Jan. 2013, San Diego, pp 616–628

Montenbruck O, Ramos-Bosch P (2008) Precision real-time navigation of LEO satellites using global positioning system measurements. GPS Solut 12(3):187–198. https:// doi. org/ 10. 1007/s10291- 007- 0080-x

Montenbruck O, Swatschina P, Markgraf M, Santandrea S, Naudet J, Tilmans E (2012) Precision spacecraft navigation using a low-cost GPS receiver. GPS Solut 16(4):519–529. https:// doi.org/ 10. 1007/ s10291- 011- 0252-6

Montenbruck O, Steigenberger P, Hauschild A (2018) Multi-GNSS Signal-in-space range error assessment—methodology and results. Adv Space Res 61(12):3020–3038. https:// doi. org/ 10.1016/j. asr. 2018. 03. 041

Montenbruck O, Hackel S, Wermuth M, Zangerl F (2021) Sentinel-6A precise orbit determination using a combined GPS/Galileo receiver. J Geodesy 95(9):109. https:// doi. org/ 10. 1007/s00190- 021- 01563-z

Murata M, Kawano I, Inoue K (2020) Precision onboard navigation for LEO satellite based on precise point positioning. In:Proceedings of IEEE/ION position, location and navigation symposium (PLANS), pp 1506–1513. https:// doi. org/ 10. 1109/PLANS 46316. 2020. 91101 58

NGA (2021) Recent update to WGS 84 reference frame and NGA transition to IGS ANTEX, National Geospatial-Intelligence Agency. https:// earth- info. nga. mil/ php/ downl oad. php? file= (U)WGS% 2084(G2139). pdf. Accessed 1 Aug 2021

Petit G, Luzum B (2010) IERS Conventions (2010), IERS Technical Note No. 36. Verlag des Bundesamtes für Kartographie und Geodäsie, Frankfurt am Main

Reichert A, Meehan T, Munson T (2002) Toward decimeter-level real-time orbit determination: a demonstration using the SAC-C and CHAMP spacecraft. In: Proceedings of ION GPS 2002, Portland, Oregon, pp 1996–2003

Rizos C, Stolz A (1985) Force modelling for GPS satellite orbits. In: Proceedinsg of 1st international symposium on precise positioning with GPS, Rockville, MD, vol 87–98

Romero I (ed) (2021) RINEX the receiver independent exchange format version 4.00, 1 Dec 2021

Roselló Guasch J, Silvestrin P, Aguirre M, Massotti L (2010) Navigation needs for ESA's Earth observation missions. In: Sandau R, Roeser HP, Valenzuela A (eds) Small satellite missions for Earth observation. Springer, Berlin, pp 439–447. https:// doi. org/10. 1007/ 978-3- 642- 03501-2_ 41

Tapley BD, Schutz BE, Born G (2004a) Statistical orbit determination. Elsevier Academic Press. https:// doi. org/ 10. 1016/ B978-0- 12- 683630- 1. X5019-X

Tapley BD, Bettadpur S, Watkins M, Reigber C (2004b) The gravity recovery and climate experiment: mission overview and early results. Geophys Res Lett 31(9):L11501. https:// doi. org/ 10.1029/ 2004G L0197 79

Toral M, Stocklin F, Bar-Server Y, Young L, Rush J (2006) Extremely accurate on-orbit position accuracy using NASA's tracking and data relay satellite system (TDRSS). In: Proceedings of 24th AIAA international communications on satellite systems conference (ICSST), pp 2006–5312. https:// doi. org/ 10. 2514/6. 2006- 5312

Wang F, Gong X, Sang J, Zhang X (2015) A novel method for precise onboard real-time orbit determination with a standalone GPS receiver. Sensors 15(12):30403–30418. https:// doi. org/ 10. 3390/s1512 29805

Won JH, Pany T (2017) Signal processing. In: Teunissen P, Montenbruck O (eds) Springer handbook of global navigation satellite systems. Springer, pp 401–442

Wu JT, Wu SC, Hajj G, Bertiger WI, Lichten SM (1993) Effects of antenna orientation on GPS carrier phase. Manuscr Geodaet 18(2):91–98

Yunck TP, Bertiger WI, Wu SC, Bar-Sever YE, Christensen EJ, Haines BJ, Lichten SM, Muellerschoen RJ, Vigue Y, Willis P (1994) First assessment of GPS-based reduced dynamic orbit determination on TOPEX/Poseidon. Geophys Res Lett 21(7):541–544. https:// doi. org/ 10. 1029/ 94GL0 0010

The paper is originally publsihed by Springer in GPS Solutions (2022) 26:12. This is republsihed here with authors' permission. *© The Author(s) 2021.*

Govt of India to launch digital crop survey in 10 states this kharif season

Government of India plans to launch a digital crop survey from the kharif-2023 season across 10 states. In the survey, information on different types of crops sown by farmers in their fields will be collected through an automated process by using "Geo-Referenced maps" of the farmland plots and remote sensing images.

The digital crop survey will be rolled out initially as a pilot project in Andhra Pradesh, Karnataka, Madhya Pradesh, Maharashtra, Odisha, Rajasthan, Tamil Nadu, Uttar Pradesh, Kerala and Gujarat, according to sources. Later, it will be gradually rolled out across the country. Once it becomes fully operational, it will add on to the age-old crop area statistics collection system, which is known as "patwari agency", that is currently in use in most of the states. According to the sources, the proposed survey will use "the latest technological advancements such as visual and advanced analytics, GIS-GPS Technologies and AI/ML" to provide "near real-time" information about the crops sown by the farmers.

"As part of the digital agriculture initiatives, the Union Ministry of Agriculture and Farmers Welfare, plans to develop a reference application for the crop-sown survey," said a source. "States to take up Geo-referencing of the village maps in their respective states." Satellite data from National Remote Sensing Centre (NRSC), which comes under the Indian Space Research Organisation (ISRO), has already been made available to the states, the source said.

Elaborating the process of the proposed survey, the source said, "A crop registry, with a list of all the crops sown in India, is being developed. The crop registry will act as a single source of truth for collecting the data in a standardized manner, during the digital crop survey." The crop registry will have ability to capture single or multiple crop IDs for the same farmland plot for the same season, along with the respective area of sowing and type of crops, such as intercrop, mixed crops, single crop,

the source said, adding that linkage to GPS and Geo-referenced Cadastral maps would enable users to reach the right farm and collect the right data and images.

The linkage to remote sensing and aerial image analysis tools can be used to cross-check data at a "larger area level" with the reported and derived information from the field level for enabling higher accuracy levels. *https://indianexpress.com*

Geospatial Excellence Centre at ISM, Dhanbad

Esri India has signed a Memorandum of Understanding (MoU) with TEXMiN Foundation to set up a Geospatial Excellence Centre at the Indian Institute of Technology (Indian School of Mines), Dhanbad. It will focus on research and innovation in spatial analytics & remote sensing for mining and exploration. Knowledge of GIS enables mining professionals to explore and calculate economic potential, manage risk, conduct environmental assessments, and analyze other concerns effectively and accurately. *https://texmin.in*

UNDP and The Ocean Cleanup team up to tackle plastic pollution

The United Nations Development Programme (UNDP) and The Ocean Cleanup have signed a Memorandum of Understanding (MoU) to collaborate on eliminating plastic pollution in oceans and rivers around the globe.

The goal of the partnership is to reduce leakages of plastics into marine ecosystems by boosting policies and behavior change aimed at advancing sound plastic waste management systems and reducing overall plastic pollution, and accelerating the deployment of interception technologies in rivers to end marine plastic pollution.

Plastic pollution poses an existential threat to the health of the world's oceans and the billions of people who depend on marine resources for food and income. Partnerships play a critical role in addressing this complex global challenge. *www.undp.org*

Sustainable monitoring of greenhouse gases

The World Meteorological Organization (WMO) initiative would create a network of ground-based measurement stations that can verify worrying air quality data that's been flagged by satellites or airplanes, potentially in the next five years.

"At present, there is no comprehensive, timely international exchange of surface and space-based greenhouse gas observations," the UN agency said, as it urged "improved (international) collaboration" and data exchange to support the 2015 Paris Agreement, which provides a roadmap for reduced carbon emissions and climate resilience.

Climate of understanding Cooperation between governments, international organizations and the private sector will be essential, if the proposed Global Greenhouse Gas Monitoring plan is to be viable, WMO has stressed. Just as important will be increased coordination between surface-based, airborne and space-based observation networks. Some governments and international organizations already carry out specific atmospheric monitoring and maintain datasets, but "there is no overall steering mechanism and there is undue reliance on research funding", WMO explained, in support of the creation of a single and internationally coordinated atmospheric monitoring body.

The Earth's atmosphere is mainly made up of nitrogen and oxygen, but there are also many different trace gases and particles that have a substantial impact on life and the natural environment.

Since industrialization, emissions of greenhouse gases have changed atmospheric composition dramatically. In particular, WMO has warned repeatedly that increasing levels of greenhouse gases such as carbon dioxide and methane are contributing to global warming and driving climate change. *https://news.un.org*

Government of Canada launches interactive mapping tool

The new Canada Marine Planning Atlas (the Atlas) - an interactive mapping tool that allows users to view and interact with data relevant to marine spatial planning has been launched recently. It includes data on economic, ecological and sociocultural activities that sometimes overlap in Canada's marine spaces.

Marine spatial planning brings together all levels of government, Indigenous partners and stakeholders to shape better the objectives and future uses of marine space. It improves ocean management by ensuring our marine spaces are used in a holistic way. The impacts of human activities are considered as well as broader ecological, economic, cultural and social considerations. Coordinating how we manage ocean activities is a key factor in achieving Canada's ambitious conservation goals of conserving 30 per cent of the world's oceans by 2030.

Tools such as the Atlas help marine spatial planners in Canada manage conservation work with human activities and industries supporting the livelihoods of many coastal communities. This is a critical part of ensuring a sustainable ocean economy for everyone. *https://www.canada.ca*

GrabMaps to power location-services for AWS in Southeast Asia

Grab has announced GrabMaps has become a data provider for Amazon Location Service, an Amazon Web Services (AWS) location-based service that is designed to help developers easily and securely add maps, points of interest, geocoding, routing, tracking, and geofencing to their applications. AWS customers, leveraging Amazon Location Service, now have access to high-quality regional mapping data that includes over 50 million addresses and points of interests (POIs) from GrabMaps spanning Singapore, Cambodia, Vietnam, Philippines, Indonesia, Malaysia, Myanmar, and Thailand. *www.grab.com*

FAA researching advanced RAIM for GPS approaches

An official evaluation of Advanced RAIM (ARAIM), a GPS technique used in aviation receivers for safer landings and take-offs, is being conducted by the William J. Hughes Technical Center (WJHTC) of the U.S. Federal Aviation Administration (FAA).

The WAAS Test Team at the technical center has begun to monitor the Integrity Support Data (ISD) parameters of ARAIM using evaluation tools and methods developed by both the center and Stanford University. Results of this monitoring will be published in a quarterly report on the WAAS Test Team website.

ARAIM addresses various weaknesses of Receiver Autonomous Integrity Monitoring (RAIM). To assure the integrity of GPS, aviation receivers implement RAIM, which detects any GPS satellite fault, and can then isolate and remove it from the navigation solution.

However, RAIM provides integrity only for horizontal operations, such as enroute and non-precision approach. Additional integrity is needed to allow advanced capabilities, such as vertically guided approaches. Other integrity systems, including the Wide Area Augmentation System (WAAS), provide the integrity needed to permit these additional operations.

Since RAIM's debut, GPS and other GNSS have evolved to improve their performance and upgraded to add an additional civilian signal, making possible ARAIM architecture.

ARAIM increases the geometric diversity and integrity availability by using two core GNSS constellations (such as GPS and Galileo). ARAIM takes advantage of the second civilian signal by specifying dual-frequency processing so that the ionospheric error from GNSS signals is directly measured by the user equipment. *www.faa.gov*

Galileo High Accuracy Service goes live!

Galileo, European Union GNSS, begins the delivery of its High Accuracy Service (HAS) as officially announced by Thierry Breton, European Commissioner for Internal Market, "feeding a prosperous market for innovative applications – from farming to drone navigation and autonomous driving."

The precise corrections provided by the Galileo HAS will allow users to improve the accuracy associated with the orbit, clocks and biases provided through the Galileo Open Service broadcast navigation messages and the GPS Standard Positioning Service navigation data. These corrections enable the computation of a high accuracy positioning solution in real-time when processed by an appropriate algorithm in the users' receivers tracking the Galileo E6-B signal.

The typical accuracy below a few decimetres (<25cm horizontal) in nominal conditions of use is a revolution where Europe provides this as an integrated service for free, thus allowing the massive development of applications worldwide. *www.gsc-europa.eu*

Inertial Labs launches updated GPS-Aided Navigation System

Inertial Labs released an upgraded version of the "INS-U" GPS-Aided Inertial Navigation System, an extended version of Differential Pressure Sensor and Embedded Air Data Computer, allowing the unit to measure airspeed with up to 600 KNOTS to enhance high dynamic applications. It can output fused (GNSS + IMU) NMEA data to Pixhawk Autopilot, which allows Pixhawk Autopilot to navigate UAV in a long-term GNSS-denied environment (more than 1 hour). Intertial Labs is a developer of GPS-Aided Inertial Navigation and Measurement Units. *https://inertiallabs.com*

Maxar awarded $192m IDIQ contract

Maxar Technologies has announced that it was awarded an indefinite delivery, indefinite quantity (IDIQ) contract by the National Geospatial-Intelligence Agency (NGA), worth up to $192 million over five years.

Under the Foreign Commercial Imagery Program contract, it will provide multiple U.S. allies and partners with commercial imagery services consisting of high-resolution electro-optical, synthetic aperture radar (SAR) and 3D data products. *www.maxar.com*

AICRAFT launched edge computing device to space

South Australian artificial intelligence (AI) company AICRAFT has successfully launched its edge computing module to set a record for Big Data processing on orbit.

The device was launched on Friday 10 February 2023 on board the JANUS-1 satellite of Antaris Space from the Satish Dhawan Space Centre of India under a commercial arrangement with NewSpace India Limited (NSIL), the commercial arm of the Indian Space Research Organisation (ISRO).

As a key sub-system of the JANUS-1 satellite, AICRAFT's edge computing module, named Pulsar, will perform ultra-fast processing of space data using artificial intelligence at lowest power consumption.

In its preliminary tests on the ground, the company has demonstrated the ability to classify 1,250 images of Earth Observation data in about 10 seconds! This was achieved using the device in low-power mode which the company expects to enable 24/7 computation, even on 'shoe-box-size' nanosatellites compared to the 10 minutes a day with current market solutions.

The module offers the advantage of being highly customisable depending on the host satellite, mission duration and orbit,

making it resilient but also affordable for a variety of customers and New Space entrants. From a software perspective, the module supports over 20 of the most popular machine learning frameworks with users able to develop algorithms for Pulsar in the same way they are developing on desktops and leveraging from open-source software. *www.spaceconnectonline.com.au*

EvoLand'– new Horizon Europe project

A consortium under the lead of VITO officially launched the new Horizon Europe project EvoLand (Evolution of the Copernicus Land Service portfolio) in Leuven (Belgium) on the 17th and 18th of January 2023. EvoLand will develop and test new and innovative methods and algorithms and implement a bundle of candidate Copernicus Land Monitoring Service prototypes. This will be realised by integrating novel EO and in-situ data with latest Machine Learning techniques to continuously monitor the status, dynamics and biomass of the land surface focussing on five key thematic domains – agriculture, forest, water, urban and general land cover.

GAF AG is part of this new research and development project that includes 10 key-players of the EU Space industry from 5 EU countries. The project will be running for the next 3 years.

Why EvoLand?

Since 2011, the Copernicus Land Monitoring Service (CLMS) provides core products for the monitoring of status and changes in vegetated and non-vegetated land cover/land use state and characteristics, biophysical variables, water and cryosphere conditions. Currently CLMS needs to advance in phase with the new Copernicus 2.0 programme, the evolving user needs, global challenges and technical capabilities, meanwhile maintaining the existing core Copernicus information products and services.

EvoLand – Evolution of the Copernicus Land Service portfolio – addresses these needs in a comprehensive way through a well-designed process, developing innovative methods, algorithms and candidate CLMS prototypes to monitor the status and changes of land use/land cover and various land surface characteristics at high spatial and temporal resolution.

How is the project going to achieve its objective?

EvoLand aims to develop eleven next-generation CLMS product candidates by integrating innovative approaches in data fusion, Machine Learning, continuous monitoring and biomass mapping, as well as through the integration of novel EO and in-situ data. In addition, the project will analyse policy, data and infrastructure requirements for the prototype services, interact with the relevant Entrusted Entities (European Environment Agency [EEA], Joint Research Centre [JRC]) and consult other main Copernicus Land stakeholders and users. *evenflow.eu*

IIT Madras, ISRO sign MoU to build AR astronaut training module

Indian Institute of Technology Madras (IIT Madras) is going to develop training module for Indian Spaceflight Program using Augmented Reality / Virtual Reality / Mixed Reality (AR / VR / MR).

Indian Space Research Organization (ISRO) would utilize the advanced technologies created at the newly-established eXperiential Technology Innovation Centre (XTIC) at IIT Madras to promote Research and Development (R&D) in the domain of Extended Reality.

A MoU was signed recently between ISRO and IIT Madras. The XTIC will not only develop XR technologies for human spaceflight program but will also impart training to concerned HSFC engineers on this technology and help in establishing a XR/VR laboratory at HSFC.

The XTIC has established 'CAVE,' a consortium of start-ups and Industries in the field of XR and Haptics in India. The ecosystem led by XTIC will be utilised for several applications ranging from Outreach and education of the Human Spaceflight Programme to Digital Twins. *https://www.iitm.ac.in*

Galaxy Onboard by Teledyne Geospatial

Teledyne Geospatial released the Galaxy Onboard, a workflow-focused solution that enables airborne surveyors to deliver quality-controlled processed data in real time. It has lowered the barrier of entry for organizations venturing into airborne mapping with a solution that does not require expertise or months of training. *teledyne.com*

Omaha Public Power District LiDAR capture for digital transformation

VeriDaaS Corporation is proud to support to the efforts of Omaha Public Power District (OPPD) in their digital transformation project.

OPPD has embarked on a massive 14-county LiDAR (Light Detection and Ranging) laser mapping program to accurately map and spatially reference all overhead electric distribution facilities. Digital transformation of a utility enhances the GIS and promotes System (GIS) and promotes the use of Advanced Distribution Management System (ADMS) leading to more efficient reliable power. *https://veridaas.com*

Lumotive and Lumentum introduce design for 3D LiDAR solutions

Lumotive, the developer of Light Control Metasurface beam steering chips enabling the next generation of 3D sensors, and Lumentum Holdings, a designer and manufacturer of innovative optical and photonic products, jointly announced the availability of the M30 Reference Design, a complete software-defined sensor implementation to enable rapid adoption of LCM-based solid-state beam steering technology. *www.lumentum.com*

DroneDeploy support for DJI Mavic 3E

DroneDeploy Flight app now supports autonomous mapping missions on the new DJI Mavic 3 Enterprise (M3E), using the RC Pro Enterprise Smart Controller. This means that, for the first time, DroneDeploy can be installed directly on your smart controller.The Mavic 3 Enterprise's high-resolution 20MP camera, support for network RTK, increased flight time and mechanical shutter make it the drone of choice for producing high-quality maps within DroneDeploy. *www.dronedeploy.com*

Automated Drones for Monitoring of Canadian Electric Power Stations

Percepto announced that Transport Canada has approved Ontario Power Generation(OPG) to operate Percepto's drone in a box solution Beyond Visual Line of Sight (BVLOS) at McConnell Lake Control Dam without a visual observer on site, a first in Canada.

A BVLOS Special Flight Operations Certificate (SFOC) was issued for the Percepto Air Max autonomous drone-in-a-box, as provided by Rocky Mountain Unmanned Systems and their GM Kevin Toderal, to perform remote inspections in a pilot project starting this month. *www.percepto.co*

TOPODRONE studies Israel floating solar farm

TOPODRONE used its synchronized lidar, airborne photogrammetry and bathymetric surveying methods to study a floating solar farm in Israel. This was completed upon request from the UAV service provider ERELIS, to help conduct a pilot project of reservoir surveying with a UAV for ETZ HADEKEL in northern Israel.

As the surface of the reservoir in Northern Israel is covered by solar panels, it is difficult to use standard methods of surveying from a boat. The goal of this study was to create 3D models, which can be used for high-precision assessments of sediment volumes, general monitoring of reservoir banks and visual monitoring. *https://topodrone.com*

Draganfly to manufacture and distribute drones in India

Draganfly Inc. has announced that Remote Sensing Instruments ("RSI has entered into a strategic agreement with Draganfly for the development of manufacturing, distribution, and sales of Draganfly products in India.

A core component of this agreement is to manufacture Draganfly drones in India under the AatmaNirbhar Bharat (Made in India) program. *www.draganfly.com*

DroneBase secures $55 million

DroneBase has secured $55 million in investment and rebranded as Zeitview. Led by Valor Equity Partners, an operational growth investment firm backing technology and technology-enabled companies, the round was followed by existing investors Union Square Ventures, Upfront Ventures, Euclidean Capital, Energy Transition Ventures, and Hearst Ventures.

The new funding will support the company's AI-enabled software and global footprint in advanced inspection solutions. *www.zeitview.com*

Regulus Cyber launches Ring – next-gen UAS system

Regulus is launching the first fully-operational, small-form-factor counter-UAS system using unique GNSS manipulation technology to defeat all UAS threats, including swarms, multi-direction attacks, dark drones, manually-piloted drones and 4G/5G drones.

In a timely development given the use of drones to attack tanks in the current conflict, this groundbreaking Ring system uses proprietary, combat-proven GNSS manipulation to take control of the drone and deflect, hold or crash it, or force it to land. *www.regulus.com*

ZF partnership with Beep

ZF unveils its next generation shuttle for autonomous driving in urban environments and mixed traffic at the 2023 Consumer Electronics Show (CES) in Las Vegas/ Nevada, USA. It has announced a strategic partnership with U.S. mobility services provider Beep, Inc. The agreement aims to deliver several thousand shuttles to customers over the coming years. *zf.com*

HERE to provide indoor/outdoor device positioning services

HERE Technologies has announced its work with Amazon Web Services (AWS) to deliver developers with improved performance for indoor/ outdoor positioning capabilities to track and manage any number of internet-of-things (IoT) devices. Recently at re:Invent 2022, AWS introduced the new AWS IoT Core Device Location feature to make it possible to track and manage IoT devices without relying on GNSS/Global Positioning System (GPS) hardware. Historically, not all IoT devices can be equipped with GPS due to its high-power requirements, larger device footprint and higher integration costs. *here.com*

World's first autonomous bus service to start operating in Scotland

CAVForth is an autonomous bus service starting this Spring, initially on a 14-mile route from Edinburgh Park transport hub, across the Forth bridge, to Ferrytoll Park & Ride in Fife. The fleet of five Alexander Dennis Enviro200AV, full sized diesel buses, will negotiate mixed traffic, and travel at speeds of up to 50mph. The 43-seater buses will carry up to 10,000 fare-paying passengers per week.

CAVForth (CAV stands for Connected and Autonomous Vehicles) is a partnership between automated technology provider and project lead Fusion Processing Ltd, bus operator Stagecoach, bus manufacturer Alexander Dennis, government agency Transport Scotland, Edinburgh Napier University, and Bristol Robotics Lab. https://edinburghguide.com

Tackling decarbonisation and improving transport resilience

The UK government has announced that a new research hub is being launched to boost innovative measures to decarbonise and improve transport, as the country works towards its net zero goals. Applications are now open for organisations to host the new hub, with the government pledging £10 million in funding for the centre, which will establish a UK centre of excellence for transport innovation.

The hub will also develop and implement innovative ideas to ensure future transport is resilient and meets the challenges of climate adaption, such as changes to weather and water levels. *www.intelligenttransport.com*

Nokia expands Lab-as-a-Service solution

Nokia is expanding its Lab-as-a-Service (LaaS) solution to include the validation testing of industrial user equipment and third-party devices connecting people and machines over Nokia digital automation cloud (DAC) and modular private wireless (MPW) networks. This will allow enterprises to streamline the testing of equipment and Industry 4.0 use cases over private wireless to assess how they will help achieve their digital transformation goals. A dedicated device testing facility in Bangalore, India will allow more customers to accelerate Industry 4.0 service adoption.

Nokia LaaS will enable enterprise customers to assess how devices and equipment working over 4.9G/LTE and 5G private wireless networks, will support their implementation of Industry 4.0 use cases. *www.nokia.com*

Orion180 integrates Nearmap

To continue improving on their underwriting process, property data and custom-score modeling, Orion180 needed a partner that could offer high quality imagery, frequently updated data, and AI derived analytics. After a selection process, they chose Nearmap as their new imagery data intelligence provider. The integration between the two partners will be delivered through a customized API. *nearmap.com*

Veteran Ventures invests with Asylon Robotics

Veteran Ventures Capital's, Veteran Fund I announced an investment into Asylon Robotics, the fastest growing, full-service, automated air and ground security robotics company in the United States. It's advanced and automated robotics systems act as significant force multipliers for streamlining security operations. The team consists of world class experts in the UAS, security, and robotics space, to include experience at Lockheed Martin, L3 Communications, Boeing Aerospace etc. *www.veteranventures.us*

Sunderland to Trial Self-driving Shuttles and Lorries

The UK city of Sunderland has received £14m in funding to deploy self-driving shuttles and lorries. The grants, part of the Centre for Connected and Autonomous Vehicles Connected and Automated Mobility programme, aim to help British companies seize early opportunities to develop experimental projects into offerings ready for the market. *www.sunderlandoursmartcity.com*

Advanced Vehicle Parking System in London

Tier Mobility has introduced a new parking system to address the issue of e-scooters being left in unsafe or obtrusive locations. E-scooter companies utilize GPS technology to locate their machines and determine designated parking zones using digital coordinates supplied by cities.

Tier Mobility has created an Advanced Vehicle Parking System (AVPS), incorporating Google's Visual Positioning System (VPS) with an in-house solution from Fantasmo. The goal of the AVPS is to accurately locate the e-scooters and validate parking spots, which have been established by many cities and councils. *www.tier.app*

USAF awards large aircraft automation study to Reliable Robotics

Reliable Robotics announced a United States Air Force contract to explore the automation of large, multi-engine jets. This study will include a feasibility assessment of full and limited aircraft automation features for cargo operations.

Remotely piloted aircraft will enable the Air Force to increase mission tempo worldwide and leverage a certifiable commercial solution for defense industry needs at fractional costs and extend aircraft capabilities. *https://reliable.co*

Kigen and Skylo collaboration

Kigen and Skylo are collaborating on satellite connectivity integration frictionless for device makers, allowing for seamless transitions between cellular and satellite connectivity via Skylo's SIM profile. This combination is particularly attractive for devices used in challenging environments, where relying on terrestrial cellular networks alone can be problematic. *kigen.com*

TEOCO expands 5G Geolocation Analytics and Optimization

TEOCO released a new version of its Mentor Suite. This latest release, v2022.2, includes enhancements to Mentor's Server, Client and CogniSense products to expand the breadth of analytics use cases with a particular focus on 5G geo-analytics and optimization using advanced machine learning algorithms.

Notable new features of the release include extending the range of geo-maps and analysis with new 5G uplink (UL) and downlink (DL) interference maps, additional 5G device capabilities analysis to support 5G network extensions activities and mobility health assurance, using 5G neighbor lists auditing. *www.teoco.com*

SBG Systems announces Quanta Plus

SBG Systems has launched Quanta Plus, its latest Inertial Navigation System (INS). It is a small, lightweight, and high-performance OEM product that can be easily integrated into survey systems with LiDAR or other third-party sensors. It is engineered to deliver accurate and reliable navigation data even in the most demanding environments. It combines a high-performance miniature tactical IMU with a GNSS receiver that is resilient to harsh covering conditions, providing RTK fixes even in challenging situations.

The system boasts a wide range of features to make it easy to use and customize for various applications. Motion profiles allow users to optimize the sensor parameters to suit different use cases, while the built-in PTP server (Precise Time Protocol) ensures sub-microsecond synchronization with external devices such as LiDAR (legacy PPS synchro still available). Additionally, Quanta Plus features a built-in datalogger, ethernet interface for seamless integration, and a user-friendly web configuration UI for simple setup and control. *sbg-systems.com*

TomTom selects Jedox

Jedox recently announced that it has been selected by TomTom for its planning and performance management needs. Challenged with disconnected Excel models and growing business complexity, TomTom identified its need to streamline and simplify their processes due to multiple data sources and an overwhelming amount of spreadsheets. *www.jedox.com*

Aero-Graphics purchase two UltraCam Eagle 4.1 aerial cameras

The first two UltraCam Eagle 4.1 aerial imaging systems to land in North America have been purchased by Salt Lake City-based Aero-Graphics Inc. Both nadir photogrammetric cameras are on track to be fully operational for the spring flying season. The 4th generation UltraCam Eagle integrates significant technological improvements, including a move to CMOS sensors, a significantly increased frame rate, and a revolutionary Adaptive Motion Compensation (AMC) feature. *vexcel-imaging.com*

UltraMap upgraded with advanced water handling features

Vexcel Imaging has released a new version of its all-in-one photogrammetric software suite UltraMap, with sophisticated and best-in-class water handling features, an enhanced Ortho module performance and a redesigned Ortho reprocessing workflow. UltraMap v6.0 introduces True Pixel Processing (TPP), a proprietary raw data processing approach in the Essentials module and supports professional data production for the recently launched UltraCam Eagle 4.1.

The new highly automated features for water handling are enhancing the quality of nearly every product throughout the workflow. This includes tools like the new Water Mask & Geometry Editor to efficiently quality-control and edit water masks as well as the updated Seamline & Blending Mask Editor for intuitive generation of homogenous water surfaces in orthomosaics. *vexcel-imaging.com*

L3Harris delivers experimental navigation satellite

L3Harris delivered the experimental Navigation Technology Satellite-3 to the Air Force Research Laboratory for its final phase of integration and testing, keeping the program on track for a late 2023 launch. AFRL announced the delivery Jan. 26, which brings the lab closer to conducting the first U.S. positioning, navigation and timing experiment in almost a half century.

AFRL awarded L3Harris an $84 million contract in 2018 to develop NTS-3, which will serve as a testbed for future GPS capabilities including steerable beams that provide regional coverage, a reprogrammable payload that can receive updates while on orbit and built-in defenses against signal jamming. The lab and the Space Force are also considering how the satellite could augment the current GPS constellation as standalone small satellites. *www.l3harris.com*

Quantum navigation research contract awarded to SandboxAQ

SandboxAQ has been awarded a Direct-to-Phase-II Small Business Innovation Research (SBIR) contract by the U.S. Air Force to research quantum navigation technologies. It will advance research and development for its quantum navigation system, which is being designed to complement the GPS for accurate navigation in degraded, contested, or denied environments where the loss of precision GPS may negatively impact operations. The company's AQ-powered quantum sensor prototype will be optimized in close coordination with the U.S. Air Force customer through a variety of identified innovation areas, including live demonstrations aboard Air Force aircraft. *www.sandboxaq.com*

GEXCEL HERON 3D Mobile Mapping

The recently released versions of GEXCEL HERON processing software(s) make HERON 3D mapping projects more accurate, effective and usable thanks to important improvements in the usage of ground control points, in the change detection workflow, and for the cloud-sharing process.

To increase Site to Sight of data efficiency, GEXCEL customers can now link up with 3DUserNet to get a special free annual subscription to the VISION platform with a direct workflow from Reconstructor to 3DUserNetVISION. This will enable users to deliver more efficiently for their customers – with the opportunity to upgrade to a full subscription at a substantial discount at any time. *gexcel.it*

Trimble technology to help power Nissan's driver assist system

Trimble has announced that Nissan Motor Co. Ltd. will use Trimble RTX® technology as its high-accuracy

positioning source, enabling the hands-off and guided freeway driving capabilities of the ProPILOT Assist 2.0* driver assistance system, available initially on the 2023 Nissan Ariya. While positioning with standard GNSS signals may drift up to 10 meters (25 feet), Trimble RTX provides higher accuracy and enables consistent lane determination for driving applications. This makes Trimble RTX a key component for many of the latest driver assistance systems like the ProPILOT Assist 2.0. Increasingly being used on freeways, lane-level accuracy via advanced driver assistance systems (ADAS), where the driver is still the ultimate decision maker, is a key enabler in the journey to fully autonomous solutions. *www.trimble.com*

OneRail leverages Trimble tech to enhance last mile logistics

Trimble and OneRail, an Orlando-based transportation technology startup focusing on last mile logistics and visibility solutions, announced the integration of Trimble Maps technology as part of OneRail's delivery platform to enhance last mile logistics. Leveraging the integration with Trimble Maps, OneRail now utilizes PC MILER commercial routing and mileage, location services, map visualization, and an advanced ETA engine to calculate and monitor deliveries in progress as well as send proactive alerts for any updates in the delivery schedule. *www.trimble.com*

Precisely acquires Transerve

Precisely has acquired Transerve, which is headquartered in the Goa region of India, provides a cloud-native location intelligence solution and data library with curated datasets, enabling fast time to value with a nimble spatial analytics SaaS solution for enterprise and midsize companies. It incorporates a simple, yet powerful, combination of geospatial artificial intelligence (AI), machine learning (ML) and geoprocessing that supports data democratization by making location analysis and data enrichment available to data-centric employees without requiring the need for GIS expertise. *www.precisely.com*

AlphaRTK announces free educational RTK access

AlphaRTK will provide students and faculty of Rutgers University, West Chester University, and Warren County Community College free access to its GNSS correction network. AlphaRTK is a privately held RTK subscription network to fully support four-constellation GNSS corrections. The service is currently available for use in New Jersey, as well as both the New York City and Philadelphia metropolitan areas.

A real-time kinematic (RTK) network is a system of ground-based stations that use data from navigation satellites to provide centimeter-accurate real-time coordinate data to users in such fields as GIS, engineering, surveying, construction etc. *www.alphartk.com*

GEODNET announces RTK, GNSS corrections service for OEMs

GEODNET announces initial availability of a Real-Time Kinematic (RTK), Centimeter Precision, GNSS Corrections Service for OEMs and Systems Integrators. It is compatible with thousands of fielded GNSS receivers from all major brands, on-vehicle automated steering and spraying kits, as well as the latest drones and robots. *https://geodnet.com*

VIAVI Solutions unveils resilient PNT

Viavi Solutions Inc. has announced the availability of the PNT-6200 Series Assured Reference for resilient positioning, navigation and timing (PNT). This solution is based on VIAVI's acquisition of Jackson Labs Technologies in November 2022, and delivers critical security for PNT to communications service providers, network equipment manufacturers, government and military, and avionics markets. The PNT-6200 Series Assured Reference provides maximum resiliency for critical infrastructure dependent on positioning and timing. It can supplement or even replace GPS signals based on connectivity to the broadest range of timing sources in the market, including Low Earth Orbit (LEO), GNSS, commercial satellite, terrestrial, wireline, and atomic clock services. *www.viavisolutions.com*

GMV assesses impact of Turkey earthquake from space

GMV is conducting an impact assessment of the earthquake that struck Turkey and Syria in the early hours of Monday, February 6. It is using optical imagery of the highest resolution to keep the EU Civil Protection Mechanism's Emergency Response Coordination Centre (ERCC) apprised of the situation facing the population and infrastructure in several affected cities (Gaziantep, İslahiye, Düziçi and Bahçe). It is assessing how the population and infrastructure have been affected by one of the largest quakes in the last decade, compiling all information from high-resolution satellite imagery. These images show the challenge faced by rescue teams and reveal the widespread destruction caused in towns and villages across the region. Completely flattened residential areas, makeshift tents set up on soccer fields, and heavy traffic jams on roads, many of which are closed, are some examples of what they have captured. *https://emergency.copernicus.eu*

Ursa Space launches Python Toolbox API on Esri ArcGIS Pro

Ursa Space Systems announced the release of a Python toolbox for satellite analytics and data ordering within Esri ArcGIS Pro.

Ursa Space leverages satellite data virtual constellation, comprising synthetic aperture radar (SAR), Optical, and radio frequency (RF) sensing from multiple commercial sources and advanced data fusion capabilities. The end product is analytic insights into physical changes on Earth. The platform orchestrates satellite imagery and analytic services at scale, to rapidly deliver insights to customers on demand. *ursaspace.com*

SUBSCRIPTION FORM

YES! I want my Coordinates

I would like to subscribe for (tick one)

☐ 1 year	☐ 2 years	☐ 3 years
12 issues	24 issues	36 issues
Rs.1800/US$140	Rs.3400/US$200	Rs.4900/US$300
*		SUPER saver

First name .....

Last name .....

Designation .....

Organization .....

Address .....

.....

City ..... Pincode .....

State ..... Country .....

Phone .....

Fax .....

Email .....

I enclose cheque no. .....

drawn on .....

date ..... towards subscription

charges for Coordinates magazine

in favour of **'Coordinates Media Pvt. Ltd.'**

Sign ..... Date .....

Mail this form with payment to:

Coordinates
A 002, Mansara Apartments
C 9, Vasundhara Enclave
Delhi 110 096, India.

If you'd like an invoice before sending your payment, you may either send us this completed subscription form or send us a request for an invoice at iwant@mycoordinates.org

***** Postage and handling charges extra.

MARK YOUR CALENDAR

March 2023

Munich Satellite Navigation Summit 2023
13-15 March
Munich, Germany
www.munich-satellite-navigation-summit.org

RIN Baska GNSS Conference (& Smart Maritime Workshop)
14-19 May 2023
Baska, Croatia
https://rin.org.uk

GEO CONNECT ASIA
15-16 March, 2023
Singapore
www.geoconnectasia.com

Drones Asia
15-16 March 2023
Singapore
https://dronesasia.com

Digital Twins 2023 (Virtual)
23 March 2023
www.digitaltwins2023.com

DGI 2023
27 Feb-01 March
London, UK
https://dgi.wbresearch.com

April 2023

GISTAM 2023
25-27 April
Prague, Czech Republic
https://gistam.scitevents.org/Home.aspx

May 2023

International Conference on Geomatics Education
10-12 May 2023
Hong Kong
www.polyu.edu.hk/lsgi/icge22/en

Geo Business 2023
17-18 May
London, UK
www.geobusinessshow.com

9th International Conference on Geomatics and Geospatial Technology
22-25 May 2023
Kuala Lumpur, Malaysia.
http://ggt2023.uitm.edu.my

FIG Working Week 2023
28 May - 01 June
Orlando, Florida, USA
www.fig.net/fig2023

June 2023

TransNav 2023
21-23 June
Gdynia, Poland
https://transnav2023.umg.edu.pl

July 2023

IGAARS 2023
16 - 21 July
Pasadena, CA, USA
https://2023.ieeeigarss.org

September 2023

Commercial UAV Expo
5-7, September 2023
Las Vegas, USA
www.expouav.com

MapmyIndia to invest in drone startup Indrones

MapmyIndia has announced that it has made a strategic investment in Indrones Solutions Private Limited (Indrones). After this investment, MapmyIndia also aims to offer customers industry-leading drones and drone-based solutions.

Indrones specializes in manufacturing drones for a variety of use cases and providing drone-based end-to-end solutions for verticals like smart cities, government, construction, oil & gas, agriculture, etc., and has developed technologies that allow for highly efficient and cost-effective data collection, data processing and analytics.

HevenDrones launches hydrogen-powered drone

HevenDrones launched its first hydrogen-powered drone for commercial use, the H2D55. With 5-times greater energy efficiency than traditional lithium battery-powered drones, the H2D55 is capable of flying for 100 minutes with a payload capacity of 7kg.

The launch of HevenDrones' hydrogen product line addresses the challenge of flight endurance and payload capacity associated with lithium battery-powered drones as well as the long term environmental impact linked to lithium mining. Without the need to frequently replace batteries, hydrogen fuel cells will also lower long term ownership costs for organizations implementing drone technology at scale. *www.hevendrones.com*

Camera for high accuracy 360° spherical image capture

Ladybug6 360-degree camera by Teledyne FLIR is a high-resolution camera designed to capture 360-degree spherical images from moving platforms in all weather conditions. It produces 72 Megapixel (MP) images with pixel values that are spatially accurate within +/- 2 mm at a 10-meter distance. *teledyne.com*

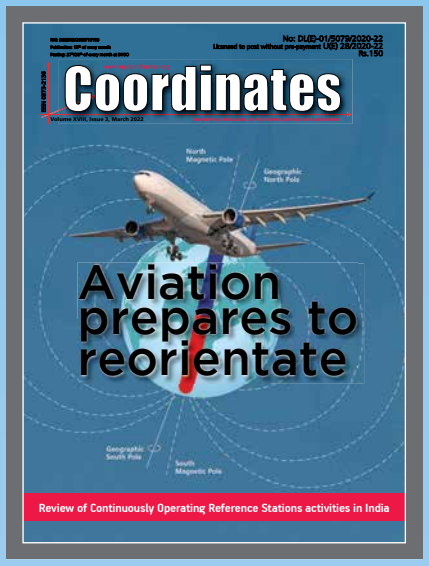

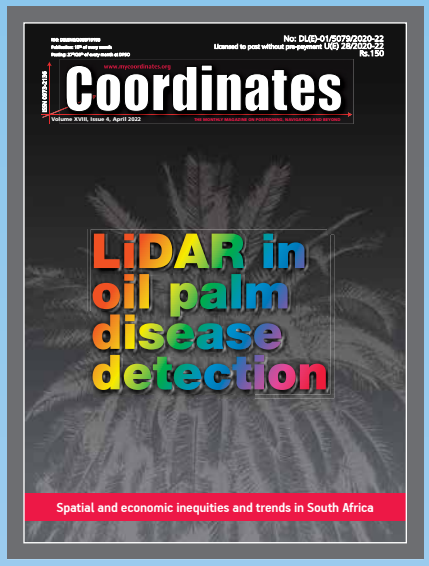

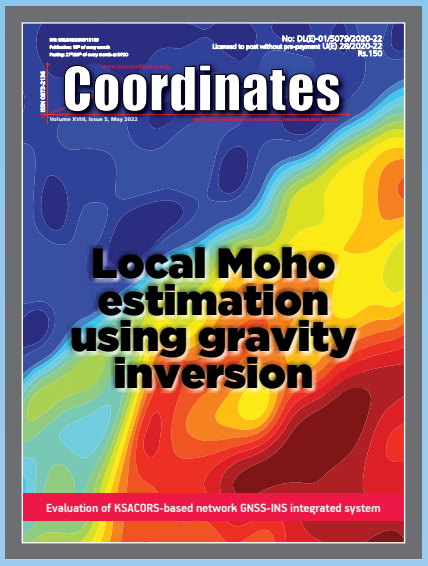

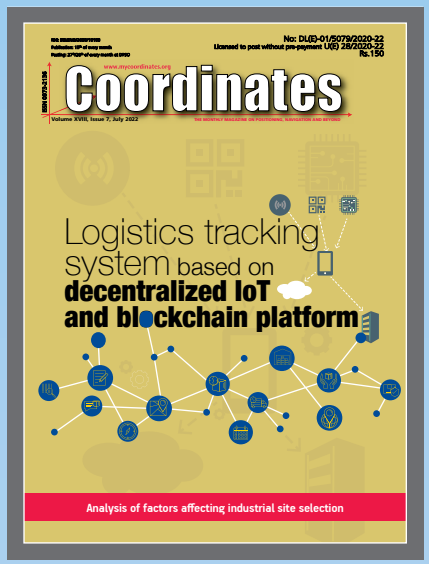

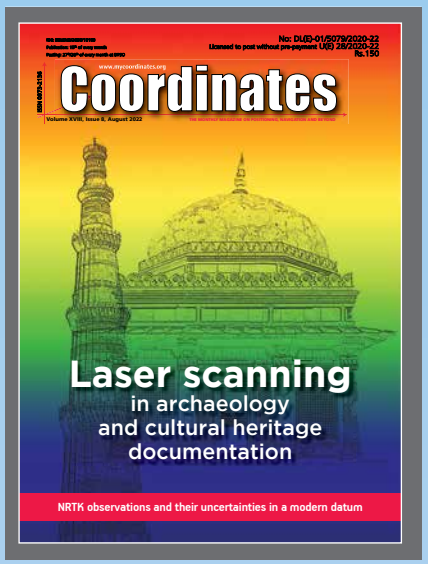

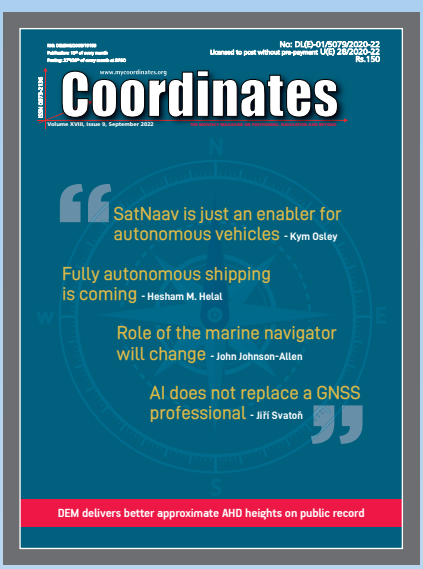

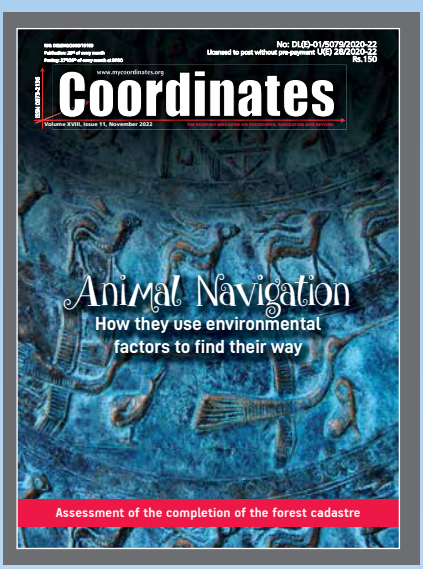

"The monthly magazine on Positioning, Navigation and Beyond"

Download your copy of Coordinates at www.mycoordinates.org

SBG SYSTEMS

0.05° ATTITUDE | **0.02°** HEADING | **1 cm** POSITION

NEW ELLIPSE-D

The Smallest Dual Frequency & Dual Antenna INS/GNSS

- RTK Centimetric Position
- Quad Constellations
- Post-processing Software

Ellipse-D
RTK Dual Antenna

Ellipse-N
RTK Single Antenna

OEM
RTK Best-in-class SWaP-C

Visit our website: **www.sbg-systems.com**